

Control Optimization – SPA II

Heaving Buoy Test Results



DOE Award Number: DE-EE0007173
Project Period: 01/01/2016 to 09-30-2018
Report Date: 6-29-17

Author

Daewoong Son

Principal Investigator

Mirko Previsic

mirko@re-vision.net

916-977 3970 ext. 200

Recipient Organization

Re Vision Consulting, LLC

1104 Corporate Way

Sacramento, CA 95831

Acknowledgment: “This report is based upon work supported by the U. S. Department of Energy under Award No. DE-EE0007173”.

Disclaimer: “Any findings, opinions, and conclusions or recommendations expressed in this report are those of the author(s) and do not necessarily reflect the views of the Department of Energy”. This document was prepared by the organizations named below as an account of work sponsored or cosponsored by the U.S. Department of Energy (DoE). Neither DoE, RE vision consulting, LLC (RE vision), any cosponsor, the organization (s) below, nor any person acting on behalf of any of them:

(A) Makes any warranty or representation whatsoever, express or implied, (I) with respect to the use of any information, apparatus, method, process or similar item disclosed in this document, including merchantability and fitness for a particular purpose, or (II) that such use does not infringe on or interfere with privately owned rights, including any party’s intellectual property, or (III) that this document is suitable to any particular user’s circumstance; or

(B) Assumes responsibility for any damages or other liability whatsoever (including any consequential damages, even if RE Vision or any RE Vision representative has been advised of the possibility of such damages) resulting from your selection or use of this document or any other information, apparatus, method, process or similar item disclosed in this document.

The views and opinions of authors expressed herein do not necessarily state or reflect those of the United States Government or any agency thereof, or RE Vision Consulting, LLC.

Proprietary Data Notice: If there is any patentable material or protected data in the report, the recipient, consistent with the data protection provisions of the award, must mark the appropriate block in Section K of the DOE F 241.3, clearly specify it here, and identify them on appropriate pages of the report. Other than patentable material or protected data, reports must not contain any proprietary data (limited rights data), classified information, information subject to export control classification, or other information not subject to release. Protected data is specific technical data, first produced in the performance of the award, which is protected from public release for a period of time by the terms of the award agreement. Reports delivered without such notice may be deemed to have been furnished with unlimited rights, and the Government assumes no liability for the disclosure, reproduction or use of such reports. This report is considered protected material in its entirety.

Document Prepared by:
RE Vision Consulting, LLC
www.re-vision.net
Project Manager: Mirko Previsic
Email Address: mirko@re-vision.net

Content

Content	3
List of Tables	5
List of Figures	6
1 Introduction	9
2 Test Objective	10
3 Test Facility	11
3.1 Wave Maker	13
4 Scaled Model Description	14
4.1 Device description	14
4.1.1 Full-scale device	14
4.1.2 Model-scale device	14
4.2 Power Take-Off description	16
4.3 Device properties	17
4.4 Froude scaling	18
5 Test Matrix and Schedule	19
5.1 Test matrix	19
5.2 Test schedule	19
6 Experimental Set Up and Methods	21
6.1 Installation	21
6.2 Instrumentation	22
7 Data Processing and Analysis	25
7.1 Data quality assurance	25
7.2 Data processing in real-time	25
7.3 Control modes	27
8 Experimental Results and Validation	28
8.1 Nomenclature	28
8.2 Numerical results	29
8.3 Free-decay test	29
8.4 Wave-excitation force	31

8.5	Power performance in regular waves.....	32
8.5.1	PTO force control	32
8.5.2	Power extraction performance results	33
Appendix A:	Specifications – motor	49
Appendix B:	Specifications – sensor	51
Appendix C:	specifications –speedgoat	52
Appendix D:	Instrumentation wiring	56
Appendix F:	Linmot-talk setting	57
Appendix G:	Test runs.....	59

LIST OF TABLES

Table 1. Specifications of OSU wave maker.....	13
Table 2. Critical properties of the buoy	17
Table 3. Froude scaling law.....	18
Table 4. Test matrix.....	19
Table 5. Test waves	19
Table 6. Testing schedule – Test Campaign I	19
Table 7. Testing schedule - Test Campaign II	20
Table 8. Testing schedule – Test Campaign III	20
Table 9. Sensors	22
Table 10. OSU wave gauge calibration slope and position.....	24
Table 11. Parameters on control panel.....	26
Table 12. Nomenclature of all variables and constant	28
Table 13. Summary of free-decay test results	31

LIST OF FIGURES

Figure 1. Overview of the DWB, OSU.....	11
Figure 2. General schematic of the DWB layout.....	12
Figure 3. Overview of the wave tank, RFS	12
Figure 4. Performance curves of the OSU wave maker	13
Figure 5. Schematic of the heaving buoy.....	14
Figure 6. Prospective view of overall system(left) and buoy (right) for 1:25 scale model	15
Figure 7. Engineering view of 1:25 scale heaving buoy	15
Figure 8. Detailed view of the transducer assembly.....	17
Figure 9. Installed device in the OSU wave basin	21
Figure 10. Installed device in the RFS wave tank.....	22
Figure 11. Calibration curve of force sensor	23
Figure 12. Layout of the installed device and probe in OSU wave basin.....	24
Figure 13. Data flow and processing steps.	25
Figure 14. Workflow of Speedgoat.	26
Figure 15. Front panel of real-time controller	27
Figure 16. Hydrodynamic coefficients in model-scale from full-scale WAMIT analysis.	29
Figure 17. Time history of the buoy position after initial position	30
Figure 18. Wave-excitation force comparison.....	32
Figure 19. Schematic of PTO control loop	32
Figure 20. Time history of motion response with different linear damping values – Test Campaign I	33
Figure 21. Time history of PTO force between input and feedback with linear damping – Test Campaign I	34
Figure 22. Time history of PTO force between input and feedback with MPC– Test Campaign I.....	34
Figure 23. Time history of displacement between simulation and measurement with MPC- Test Campaign I	35
Figure 24. Time history of velocity between simulation and measurement with MPC – Test Campaign I	35
Figure 25. Time history of absorbed power between simulation and measurement with MPC – Test Campaign I	36
Figure 26. Time-averaged power performance with MPC – Test Campaign I.....	36
Figure 27. Heave response amplitude of operator for different linear damping - Test Campaign II ...	37
Figure 28. Time history of PTO force between input and feedback with linear damping - Test Campaign II	38
Figure 29. Linear damping optimization - Test Campaign II	38
Figure 30. Performance with linear damping in time series - Test Campaign II.....	39
Figure 31. Performance with causal control in time series - Test Campaign II.....	39
Figure 32. Performance with MPC in time series - Test Campaign II.....	40
Figure 33. Time-averaged power performance - Test Campaign II	40
Figure 34. Linear damping optimization - Test Campaign III	41
Figure 35. Optimal linear damping for each wave period	42

Figure 36. Performance for linear damping in time series - Test Campaign III 42

Figure 37. Performance for causal control in time series - Test Campaign III 43

Figure 38. Performance for linear MPC in time series - Test Campaign III 43

Figure 39. Position comparison between simulation and experiment with MPC – Test Campaign III. 44

Figure 40. Velocity comparison between simulation and experiment with MPC - Test Campaign III . 44

Figure 41. PTO force comparison between simulation and experiment with MPC - Test Campaign III
..... 45

Figure 42. Power comparison between simulation and experiment with MPC - Test Campaign III 45

Figure 43. Time-averaged power performance - Test Campaign III 46

Figure 44. Heave response amplitude of operator - Test Campaign III 46

Figure 45. Performance with optimal linear damping in irregular waves 47

Figure 46. Performance with MPC in irregular waves 48

This page intentionally left blank

1 INTRODUCTION

This testing program measures the performance of a 1-DoF heaving wave-energy converter device to validate control strategies as part of our efforts under our SPA-II project to develop optimal controls approaches.

The core objectives of this project is to improve the power capture of three different wave energy conversion (WEC) devices by more than 50% using an advanced control system and validate the attained improvements using wave tank and full scale testing. In parallel, we will bring along the development of a wave prediction system that is required to enable effective control and test it at full scale. Development efforts will start at a TRL 3 and end at a TRL6.

The purposes of this report are to:

- Plan and document the 1/25th scale device testing at the wave-tank facility;
- Document the test article, setup and methodology, sensor and instrumentation, mooring, electronics, wiring, and data flow and quality assurance;
- Communicate the testing results between the associated members;
- Facilitate reviews that will help to ensure all aspects (risk, safety, testing procedures, etc.);
- Provide a systematic guide to setting up, executing and decommissioning the experiment.

2 TEST OBJECTIVE

The main objective of the 1/25th scale point-absorber type heaving buoy is to obtain the necessary measurements required for validate the performance of different control strategies. This includes:

- Validate the hydrodynamic coefficients such as wave-excitation force, radiation damping, drag coefficient of the device;
- Validate the numerical results from WAMIT;
- Measure the power-extraction performance of the WEC device with different control strategies (Linear damping, Causal control, MPC).

3 TEST FACILITY

Testing was mainly conducted in the Directional Wave Basin (DWB) at O. H. Hinsdale Wave Research Laboratory of Oregon State University (OSU), Corvallis, Oregon. The DWS is an indoor basin having an overall length of 48.8 m (160 ft.), a width of 26.5 m (87 ft.) and a depth of 1.37 m (4.5 ft.). A photo of the DWB can be found in Figure 1. The basin has an instrumentation carriage spanning the width of basin. The opposite end of wavemaker is 1:10 removable steel beach. Uni-strut inserts are placed in rows with 1.2 m spacing to affix wave gauge and model in floor of the basin. Figure 2 shows general schematic of the DWB layout.

The second testing was performed in the Richmond Field Station (RFS) of University of California at Berkeley, which is shown in Figure 3. The RFS wave-tank has 68 m length, 2.4 m width, and 1.8 m depth with a flap-type wave maker. A carriage can travel along with the length of the tank.



Figure 1. Overview of the DWB, OSU

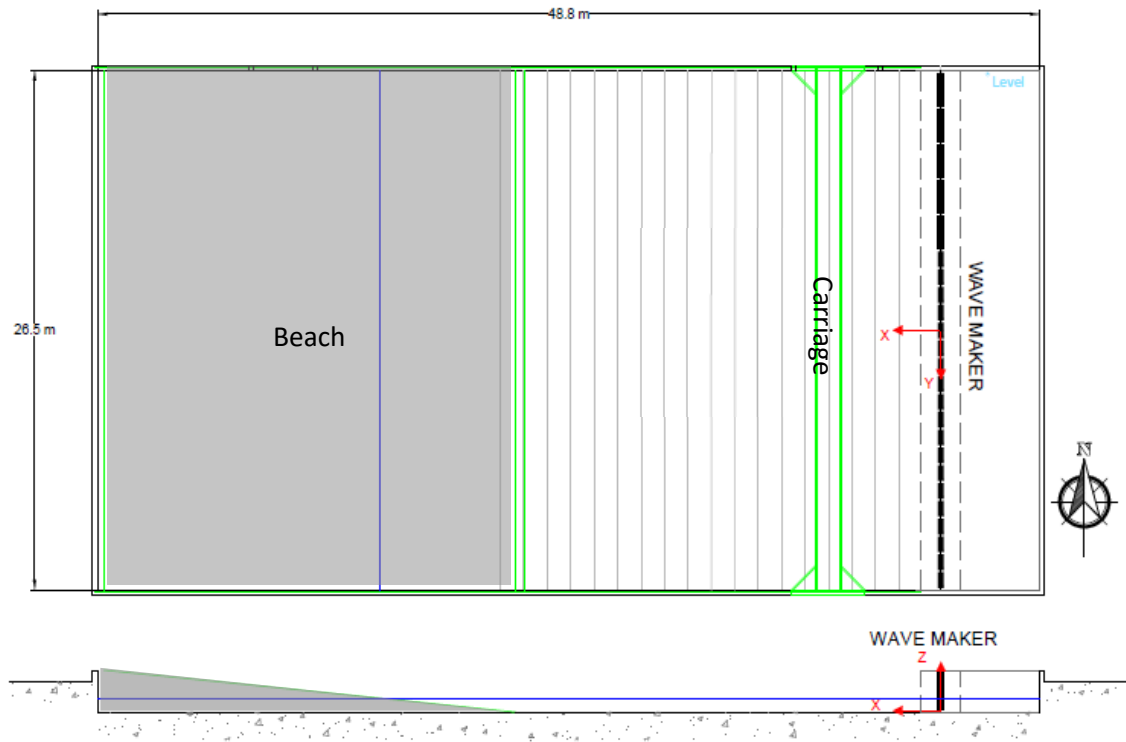


Figure 2. General schematic of the DWB layout

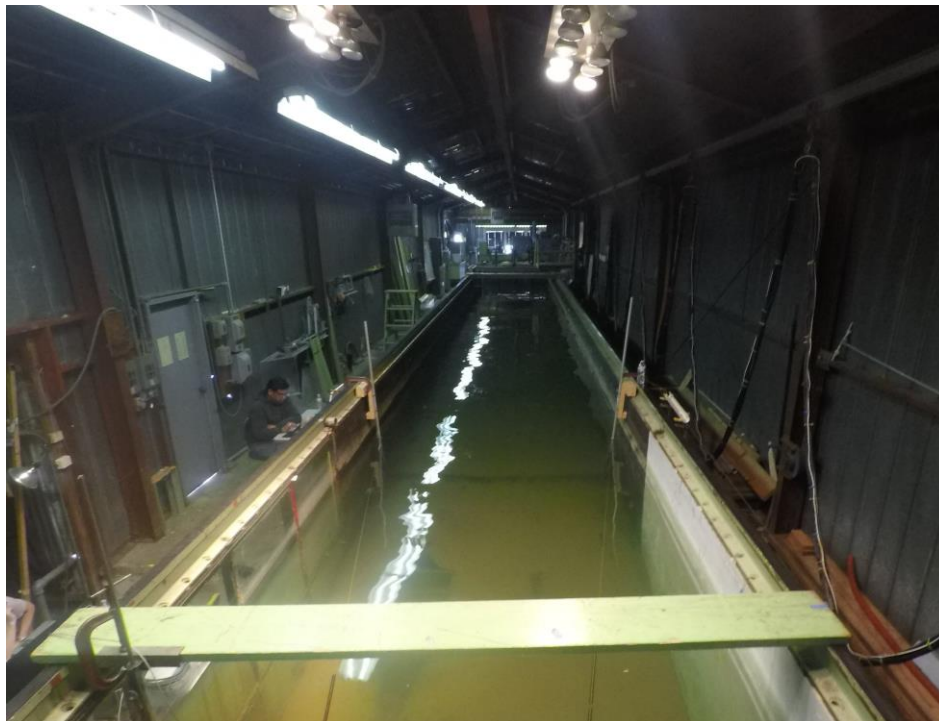


Figure 3. Overview of the wave tank, RFS

3.1 WAVE MAKER

The OSU wave maker is a piston-type system made of 29 boards with up to 2.1 m long stroke. The 29 boards of 2 m (6.6 feet) height are driven by electrical motors. The facility has been designed to generate regular, irregular, Tsunami and multidirectional waves. Detailed specifications of the OSU wave maker are list in Table 1.

Table 1. Specifications of OSU wave maker

Parameter	Value
Period range	0.5 to 10 sec
Max. wave	0.75 m (2.5 ft.) in 1.37 m (4.5 ft.) depth
Max. stroke	2.1 m (6.9 ft.)
Max. velocity	2.0 m/s (6.6 ft./s)

Figure 4 shows the performance curves of the OSU wave maker as functions of wave height (h)/water depth (H) and wave height (h)/wave length (L). Based on this performance curves, wave conditions, i.e., periods and height, were selected to retain linear-wave theory.

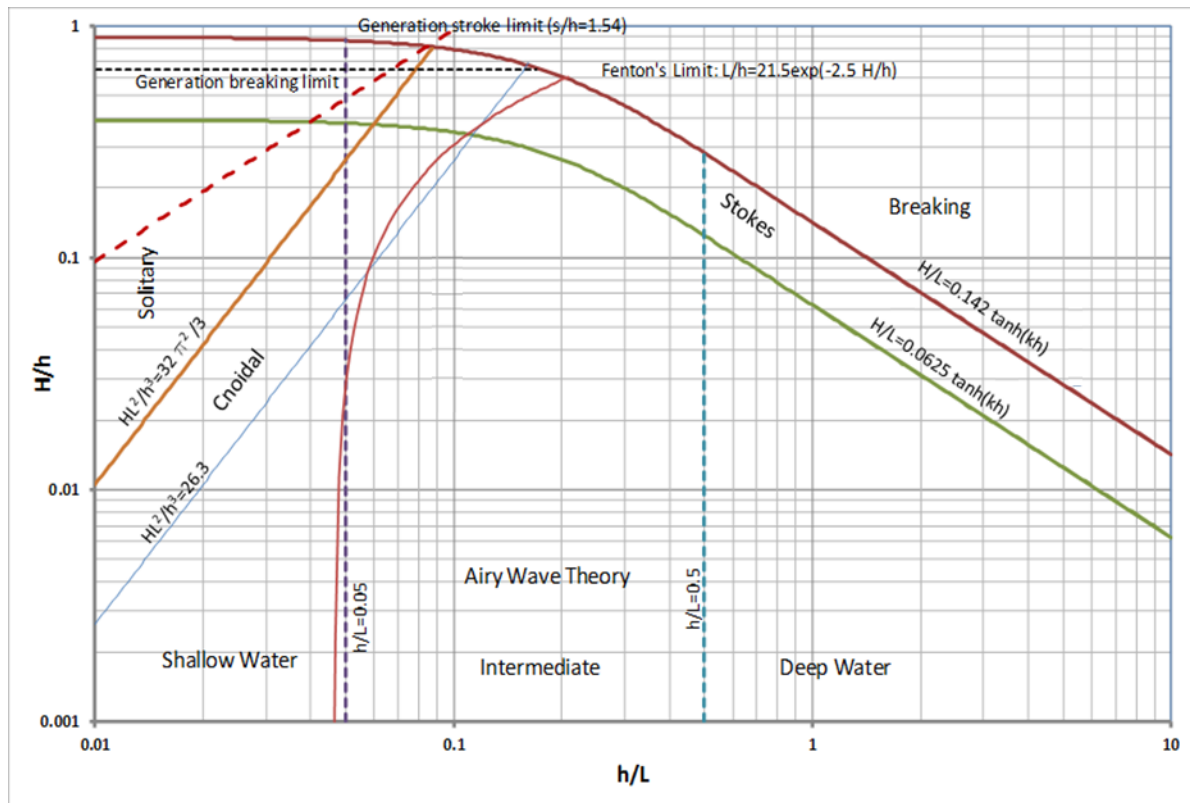


Figure 4. Performance curves of the OSU wave maker

4 SCALED MODEL DESCRIPTION

4.1 DEVICE DESCRIPTION

4.1.1 Full-scale device

The heaving buoy designed by RE Vision Consulting, LLC., is a heaving point-absorber wave-energy converter (WEC). A single body is constrained to move vertically in response to incident waves. The relative vertical motion with respect to the fixed structure or platform is utilized to capture wave energy. The buoy has an axisymmetric body, with conical bottom shape. The general concept of the heaving buoy is illustrated in Figure 5.

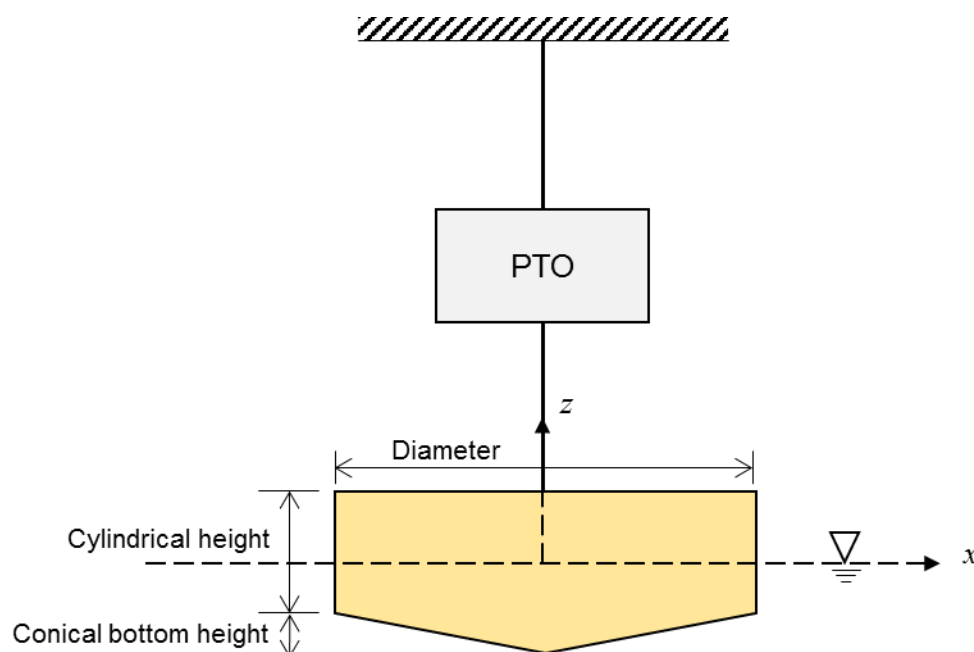


Figure 5. Schematic of the heaving buoy.

The full-scale device is expected to be deployed in intermediate or deep water, and dimensions are a diameter of 11 m, a cylindrical height of 4 m, and conical bottom height of 1.2 m (30% of the cylindrical height).

4.1.2 Model-scale device

For testing in the wave basin, the device was scaled down by 25X from the full-scale design. A SolidWorks rendered image of the 1:25 scale model and proposed arrangement for testing at wave tank are shown in Figure 6. An engineering view of the heaving buoy is also shown in Figure 7.

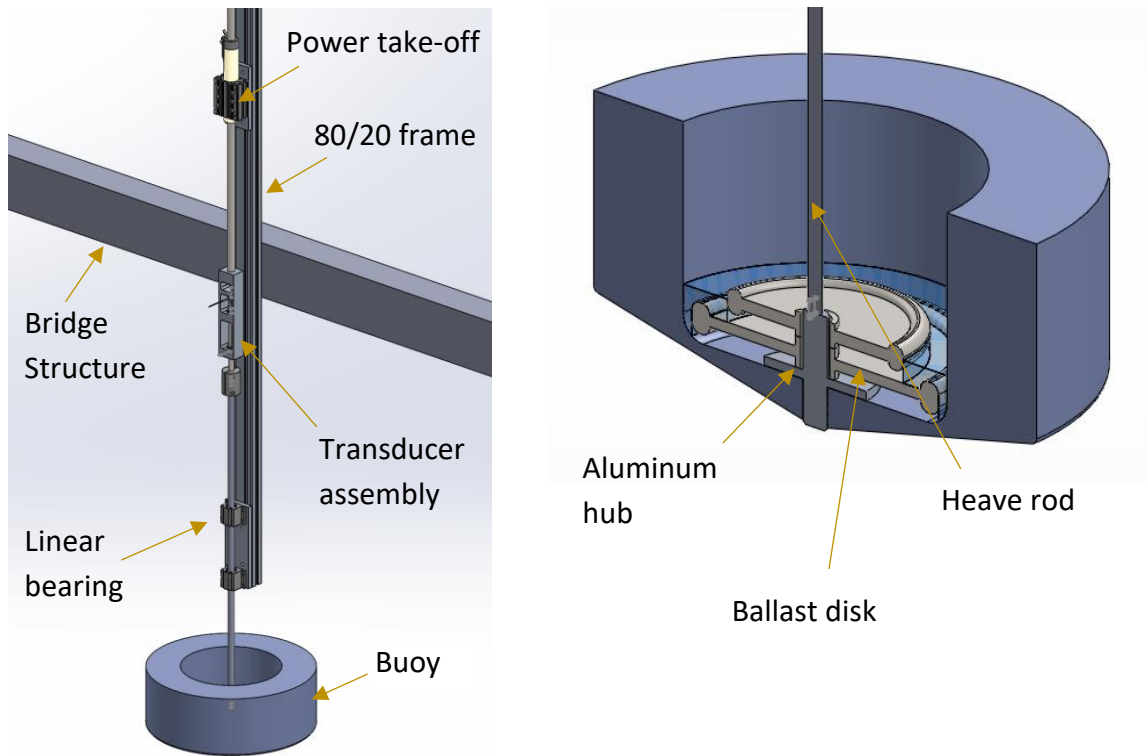


Figure 6. Prospective view of overall system(left) and buoy (right) for 1:25 scale model

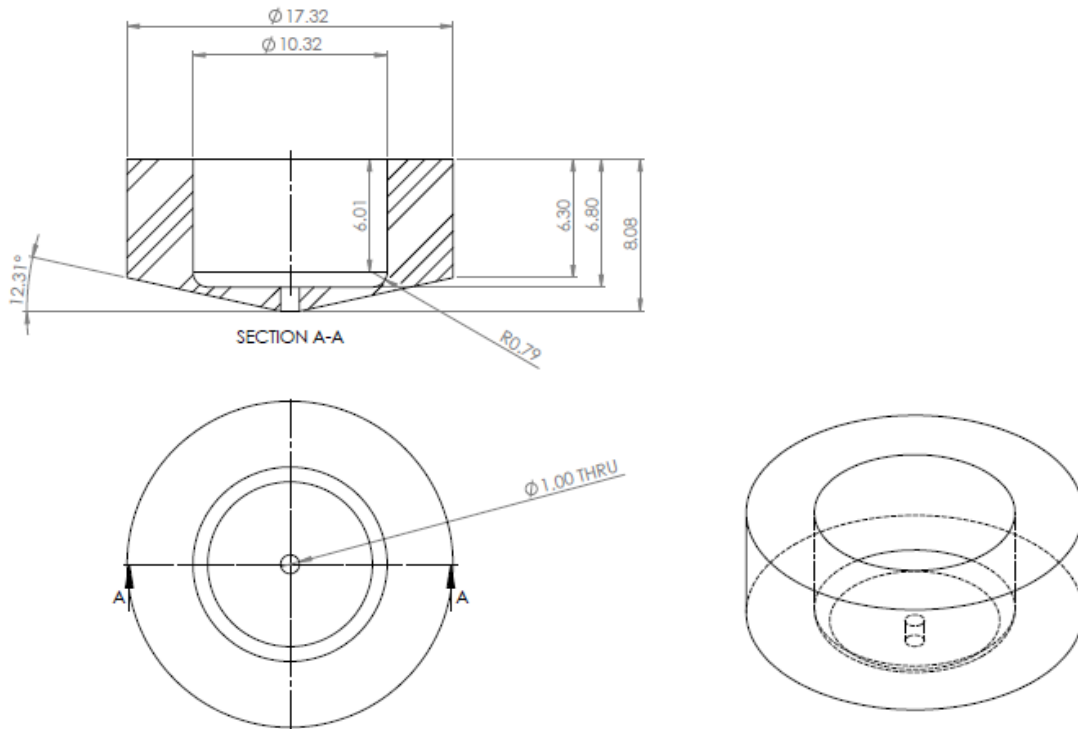


Figure 7. Engineering view of 1:25 scale heaving buoy

The elements of the model-scale WEC device for tank testing are as follows:

- The buoy: moving part of the device made by Foam and Fiberglass for surface;
- The power take-off: permanent magnet linear motor consisting of stator and slider;
- The transducer assembly: contains a load cell and connects the slider to the heave rod;
- The ballast disk: weights to match desired draft of the buoy, 15 lbs (6.8 kg);
- The heave rod: (1) 8" (length) x 0.5" (diameter) shaft for compatibility with load cell carrier;
(2) 36" (length) x 0.625" (diameter) shaft connected to the center of buoy.

The power take-off and linear bearings for heave rod are mounted on 80/20 frame, which is attached to the platform or carriage using C-clamps.

4.2 POWER TAKE-OFF DESCRIPTION

The power take-off (PTO) is a direct-drive permanent magnet linear motor PS01x37-120C with PL01-20x1600/1520-LC slider manufactured by LinMot. It provides a maximum 163 N reaction force. Specifications of motor and drive is included in [Appendix A](#).

The moving part of magnet or slider is connected to the buoy, while the stator is mounted on the bridge. The motor force is controllable via an analog signal provided by the motor drive which allows real-time force control loops to be implemented. The load cell is positioned between the slider and the heave rod as shown in Figure 8, thus measuring the total linear force between the buoy and the PTO. Linear bearings isolate the forces transferred to the load cell to 1-DoF and insure off-axis loads.

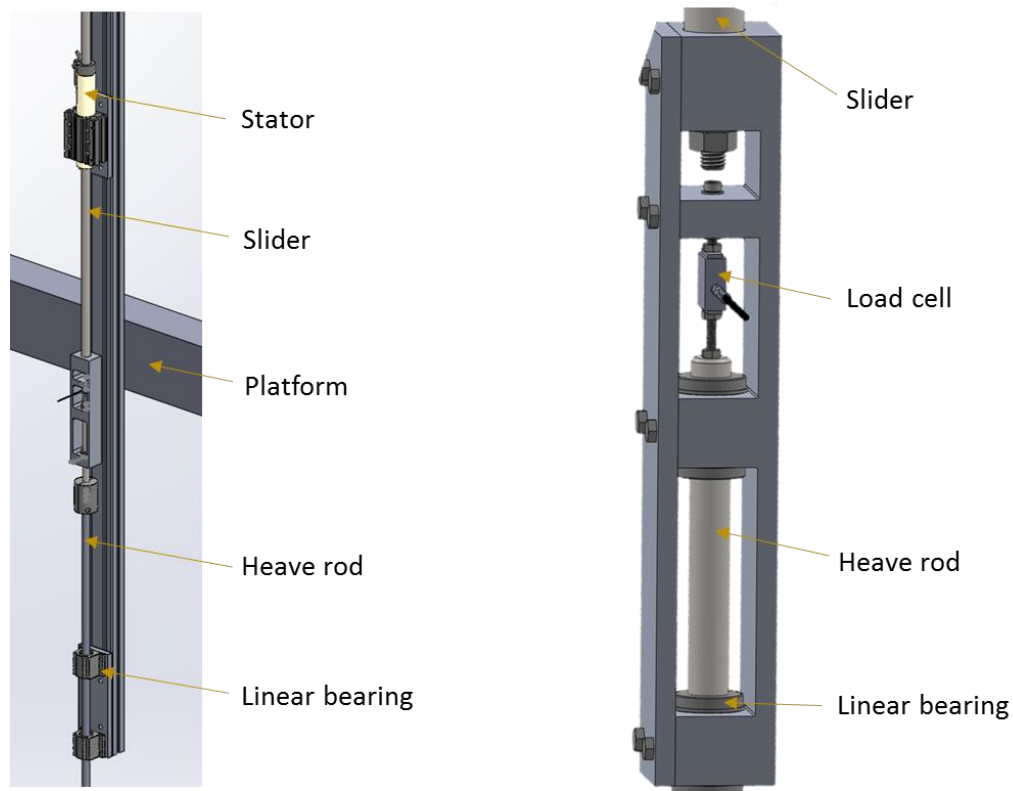


Figure 8. Detailed view of the transducer assembly

The motor drive provides position measurements in form of a simulated encoder output. A encoder to voltage converter manufactured by Laurel Electronics, provides the user scalable analog output 0-10V from digitally transmitted pulse counts.

4.3 DEVICE PROPERTIES

The full-scale and 1:25th model-scale buoy properties are listed in Table 2. Definition of geometrical parameters of the buoy is shown in Figure 5.

Table 2. Critical properties of the buoy

	Full-scale	Model-scale
Diameter (m)	11	0.44
Cylindrical height (m)	4	0.16
Conical bottom height (m)	1.2	0.048
Draft (m)	3.2	0.128

Water depth (m)	35	1.365
Displaced mass (kg)	228079.6	14.60
Submerged volume (m ³)	228.08	0.146

4.4 FROUDE SCALING

Device linear dimensions and properties are scaled per Froude scaling laws, listed in Table 3 below.

Table 3. Froude scaling law

Quantity	Units	Scaling
Wave height and length	m	S
Wave period and time	sec	$S^{0.5}$
Wave frequency	Hz	$S^{-0.5}$
Linear displacement	m	S
Linear velocity	m/s	$S^{0.5}$
Force	N	S^3
Power	W	$S^{3.5}$
Mass	Kg	S^5
Linear stiffness	N/m	S^2
Linear damping	N/(m/s)	$S^{-2.5}$

5 TEST MATRIX AND SCHEDULE

5.1 TEST MATRIX

The performed tests of the 1/25th scale device at wave-tank listed in Table 4, and incident-wave conditions for testing are shown in Table 5. Detailed test runs are listed in [Appendix G](#).

Table 4. Test matrix

ID	Tests	Measurements	Device	Wave
1	Free-decay	. Position		-
2	Wave-excitation force	. Force . Incident-wave elevation	Fixed	Regular
3	Power performance	. Force . Position . Incident-wave elevation	-	Regular

Table 5. Test waves

Type	Period	Height	Test ID
Regular	1.0/1.4/1.8/2.2/2.6/3.0/3.4 sec	4 cm	2. 3
	5/7/9/11/13/15/17 sec	1 m	(Full scale)
h/L (OSU)	0.87/0.45/0.28/0.21/0.17/0.14/0.12	0.03 (H/h)	

5.2 TEST SCHEDULE

TEST CAMPAIGN I was carried out at the Oregon State University (OSU) tank facility from March 6 (Monday) to March 8 (Wednesday), 2017, as shown in Table 6.

Table 6. Testing schedule – Test Campaign I

Date/Time	Event
Monday	WEC installation and work-in
08:00 – 14:00	Assembling and installation of the device, set up for testing and verifying operation
14:00 – 17:00	Force control loop debugging

Tuesday	Full Test Day
08:00 – 15:30	Force control loop debugging
15:30 – 17:00	Wave-excitation force test
Wednesday	Full Test Day
08:00 – 08:30	Free-decay test
08:30 – 10:00	Wave-excitation force test
10:00 – 17:00	Performance test in regular waves with linear damping and MPC

TEST CAMPAIGN II was carried out at the Richmond Field Station (RFS) of the UC Berkeley from April 19 (Wednesday) to April 21 (Friday), 2017, as shown in Table 7.

Table 7. Testing schedule - Test Campaign II

Date/Time	Event
Wednesday	WEC installation
18:00 – 20:00	Assembling and installation of the device, set up for testing and verifying operation
Thursday	Full Test Day
09:00 – 15:30	Performance test in regular waves with linear damping
15:30 – 20:00	Performance test in regular waves with MPC
Friday	Full Test Day
09:00 – 14:00	Performance test in regular waves with MPC
14:00 – 19:00	Performance test in regular waves with Causal control
19:00 – 21:00	Decommissioning the model

TEST CAMPAIGN III was carried out at the OSU from May 24 (Wednesday) to May 26 (Friday), 2017, as shown in Table 8.

Table 8. Testing schedule – Test Campaign III

Date/Time	Event
Wednesday	WEC installation and work-in
12:00 – 15:30	Assembling and installation of the device, set up for testing and verifying operation
15:30 – 17:00	Performance test in regular waves with linear damping
Tuesday	Full Test Day
08:00 – 11:00	Performance test in regular waves with MPC
11:00 – 12:00	Performance test in regular waves with Causal control
12:00 – 17:00	Performance test in regular waves with linear damping
Wednesday	Full Test Day
08:00 – 11:00	Performance test in regular waves with Causal control
11:00 – 16:30	Performance test in regular waves with MPC
16:30 – 17:30	Decommissioning the model

6 EXPERIMENTAL SET UP AND METHODS

6.1 INSTALLATION

The slider, transducer assembly, and heave rod need to be connected sequentially. Figure 9 and Figure 10 show the installed device in the Oregon State University (OSU) wave basin and the Richmond Field Station (RFS) wave tank, respectively. One of wave gauges is aligned with the center of buoy, and another one is positioned the device ahead.

After installing the device in wave tank, a fundamental functionality test should be done to check force control mode of LinMot motor and to confirm direction of the force and position. The positive PTO force moves the buoy up (positive position).

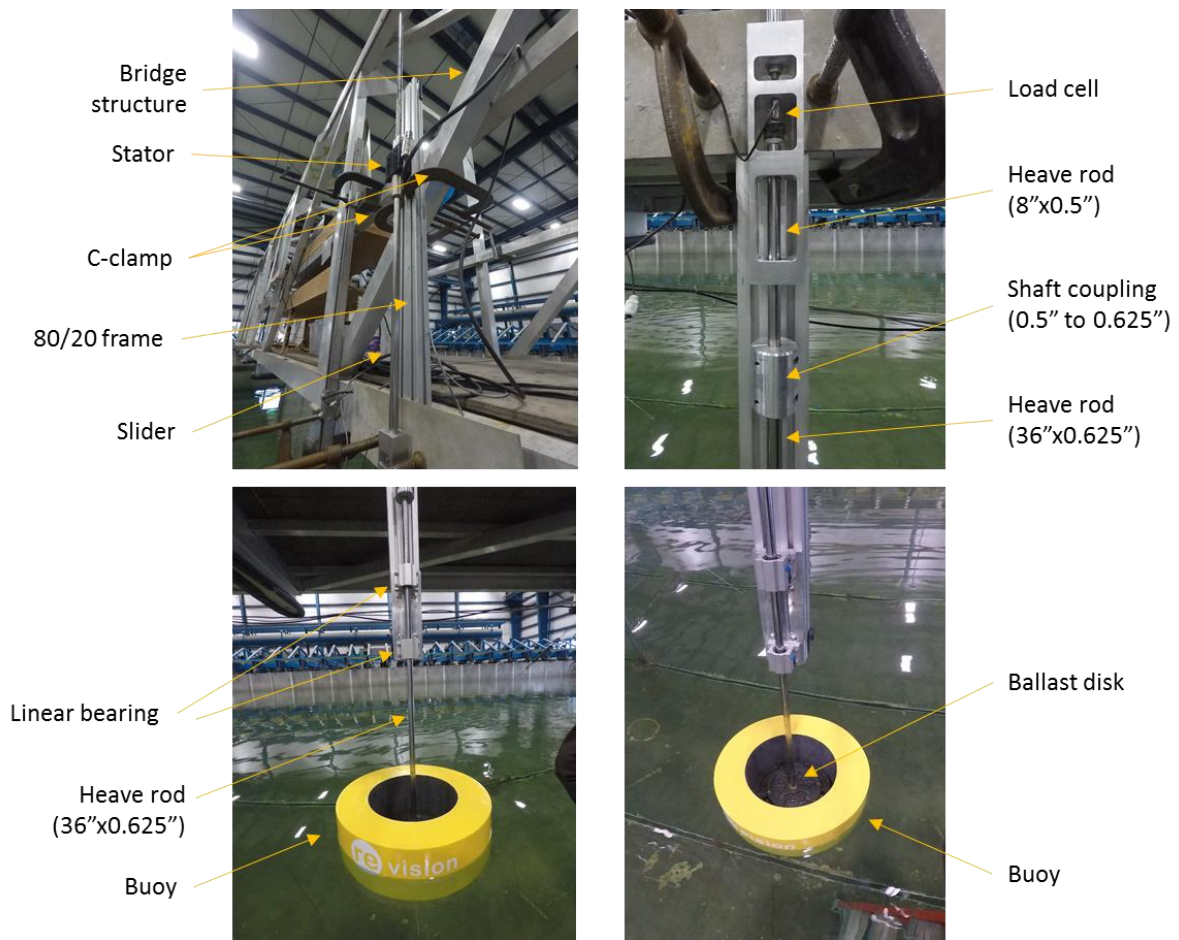


Figure 9. Installed device in the OSU wave basin

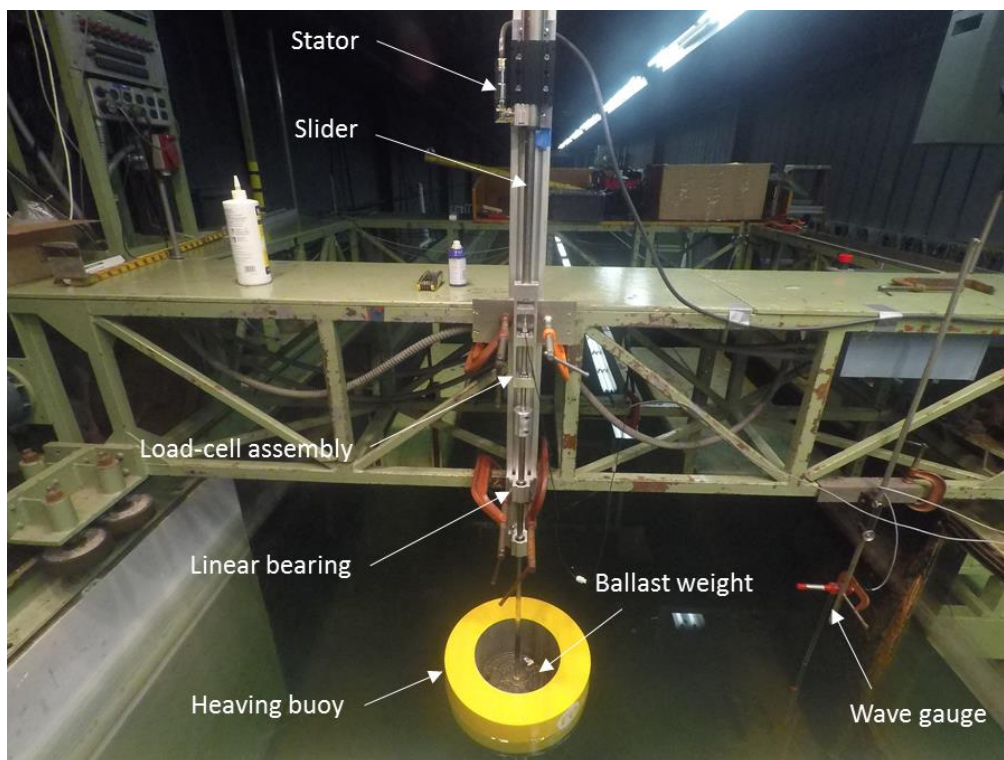


Figure 10. Installed device in the RFS wave tank

6.2 INSTRUMENTATION

The sensors used for testing are listed in Table 9 below:

Table 9. Sensors

Function	Sensor	Maker	Units
PTO force	LSB200 – 50lb	Futek	N
Linear position	LT61QD	Laurel Electronics, Inc.	m
Wave elevation	Twin-wire resistance wave gauge (OSU) Capacitance wave gauge (RFS)	-	m

The following points should be noted in relation to the interface with sensor systems:

- Force feedback is provided by way of a dedicated load cell, which is connected to a strain gauge amplifier manufactured by Mantracourt Electronics. An output in volts from the sensor is provided in the calibration curve, which is shown in Figure 11. Detailed information of the load cell and amplifier is included in [Appendix B](#).

- Linear position is provided by way of a simulated quadrature encoder outputs, providing A/B/Z TTL signals from the LinMot drive. The connected Laurel transmitter provides analog output for position from quadrature encoder signal by digital-to-analog converter. To scale analog output, two endpoints of output range needs to be set. After calibration, a slope of -11.913 mm/V was used at +/- 3000 count range of the encoder, with 10 um resolutions.
- OSU provided the wave gauge of twin-wire resistance type. Seven wave probes were installed around the device in semicircle as shown in Figure 12. The provided conversion slope between the voltage output and wave elevation in meter is listed in Table 10. At the RFS facility, wave gauges of capacitor type were installed with 18.05 m distance between them. In addition, wave maker signal is also provided, which is 5 volts from 0 volt when it starts.

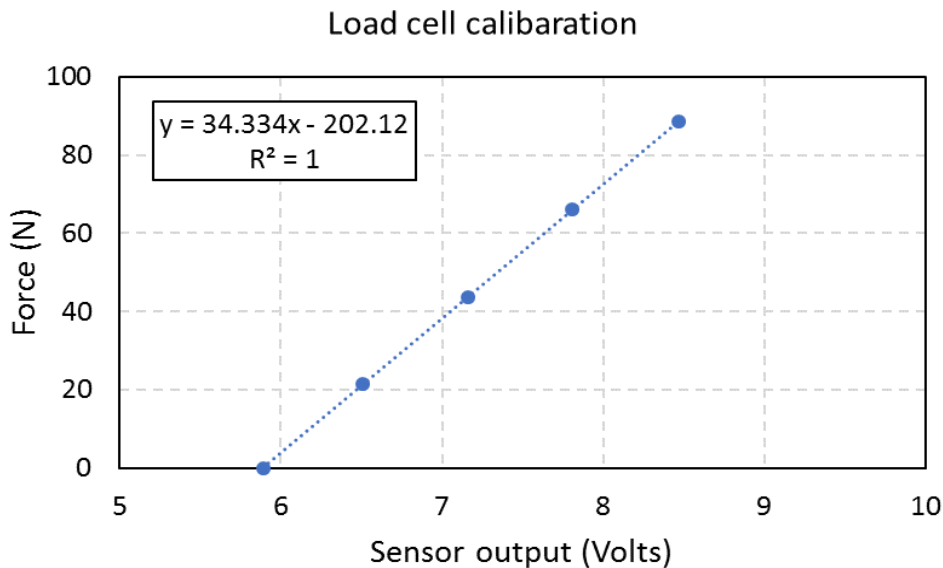


Figure 11. Calibration curve of force sensor

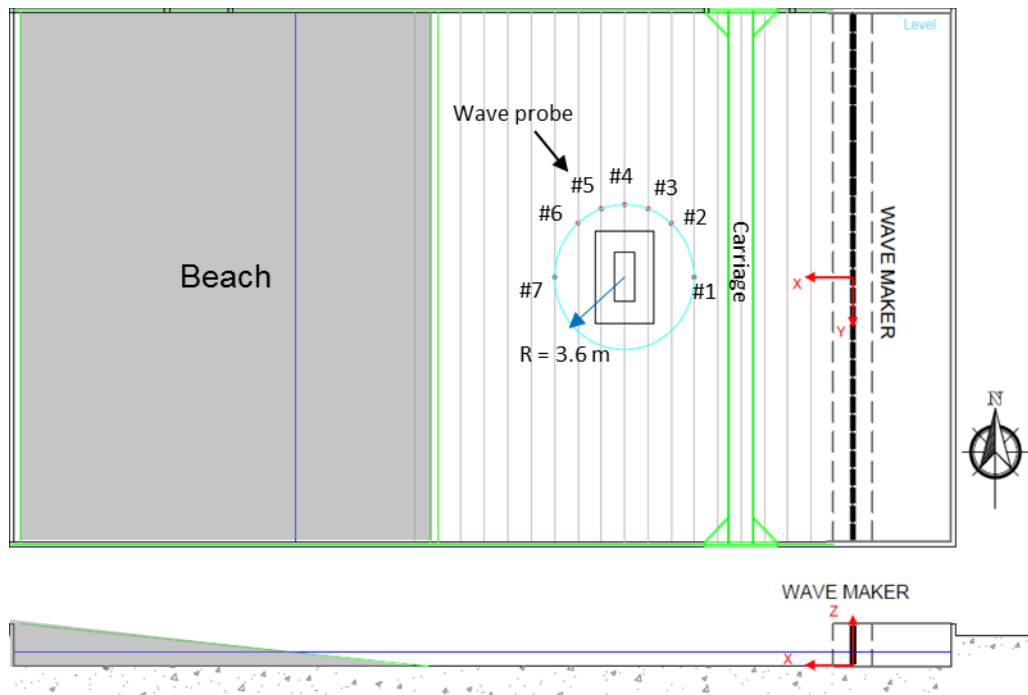


Figure 12. Layout of the installed device and probe in OSU wave basin

Table 10. OSU wave gauge calibration slope and position

Wave probe #	Slope	Slope unit	X-Position (m)	Y-Position (m)
1	0.231	m/V	9.477	0.003
2	0.228	m/V	10.704	2.687
3	0.227	m/V	11.909	3.427
4	0.346	m/V	13.141	3.624
5	0.228	m/V	14.351	3.414
6	0.239	m/V	15.574	2.697
7	0.230	m/V	16.779	-0.006

7 DATA PROCESSING AND ANALYSIS

7.1 DATA QUALITY ASSURANCE

Data collection started just before wave maker started and continued until wave generation stopped. This ensure that the data captures the initial conditions and ramp-up/down as well as the trigger signal to enable subsequent time synchronization.

Raw data from the wave gauges and from the sensors were collected by the same data acquisition system and stored in a .mat file for each test run. The data quality assurance was checked at three points: 1) visually in real-time during each test, 2) in-between test runs through the initial processing, and 3) data analysis after testing. Corrective action was taken if any issues in the data and device were observed.

7.2 DATA PROCESSING IN REAL-TIME

The data flow and processing steps are shown in Figure 13. The tests were performed using pre-written scripts that run on a Speedgoat system. These scripts load the data, perform initial processing, and create figures for review. Post-processing and analysis were completed using achieved data file after testing was complete.

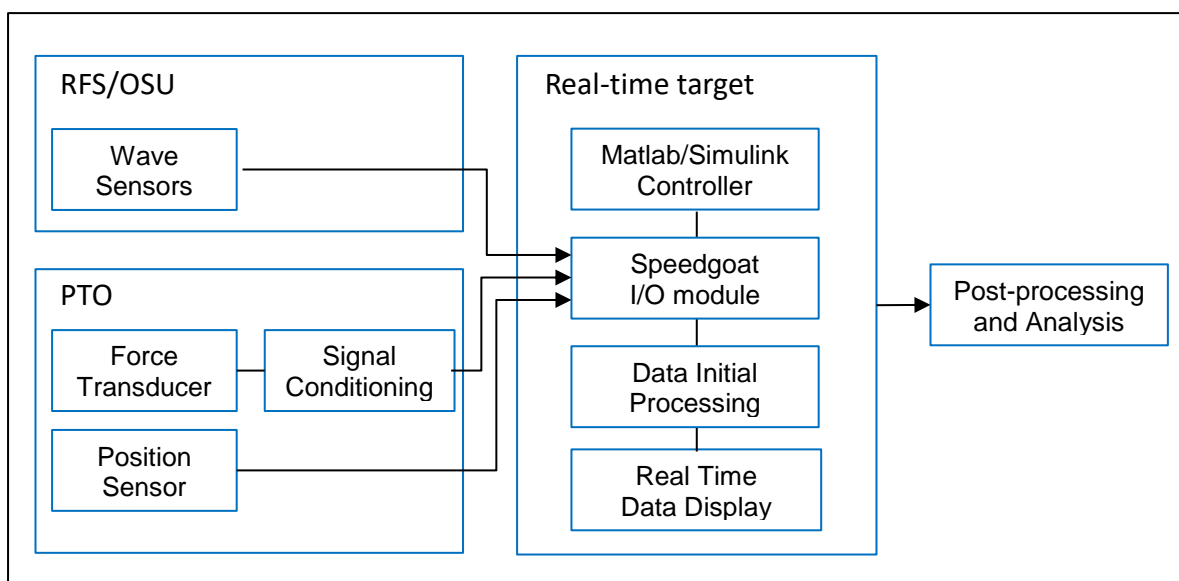


Figure 13. Data flow and processing steps.

For real-time data assessment and control prototyping, Speedgoat was used. Speedgoat is a real-time target machine that allowed us to execute Simulink models in real-time. Specifications of the Speedgoat system is included in [Appendix C](#). This Speedgoat system allows live parameter tuning, signal monitoring and execution control. Workflow of the Speedgoat system is illustrated in Figure 14. Wiring to sensors via I/O module of the Speedgoat is illustrated in [Appendix D](#).

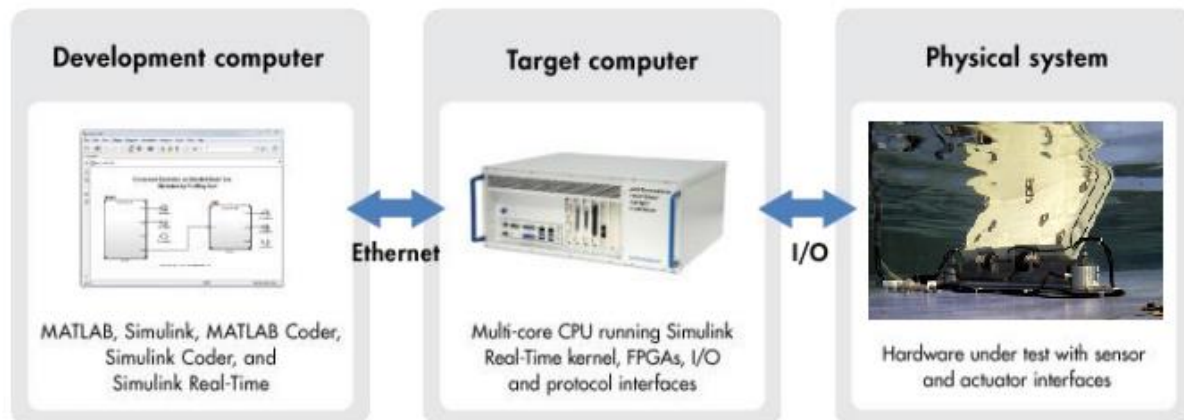


Figure 14. Workflow of Speedgoat.

A screen-shot of the front panel for real-time data processing and different control mode is provided in Figure 15. It should be noted that all input values from control panel should be full-scale values, and are then converted into model-scale values in Simulink. The parameters implemented on the front panel as follows:

Table 11. Parameters on control panel

Parameter	Description	Units
Control Modes	1: Linear damping, 2: Causal control, 3: Safe damping, 4: MPC	
Set loop gain	Loop gain for all control modes	
Damper	Used to set PTO damping value for linear damping (Test 5)	N/(m/s)
Safe damper	PTO damping value for safe operation	N/(m/s)

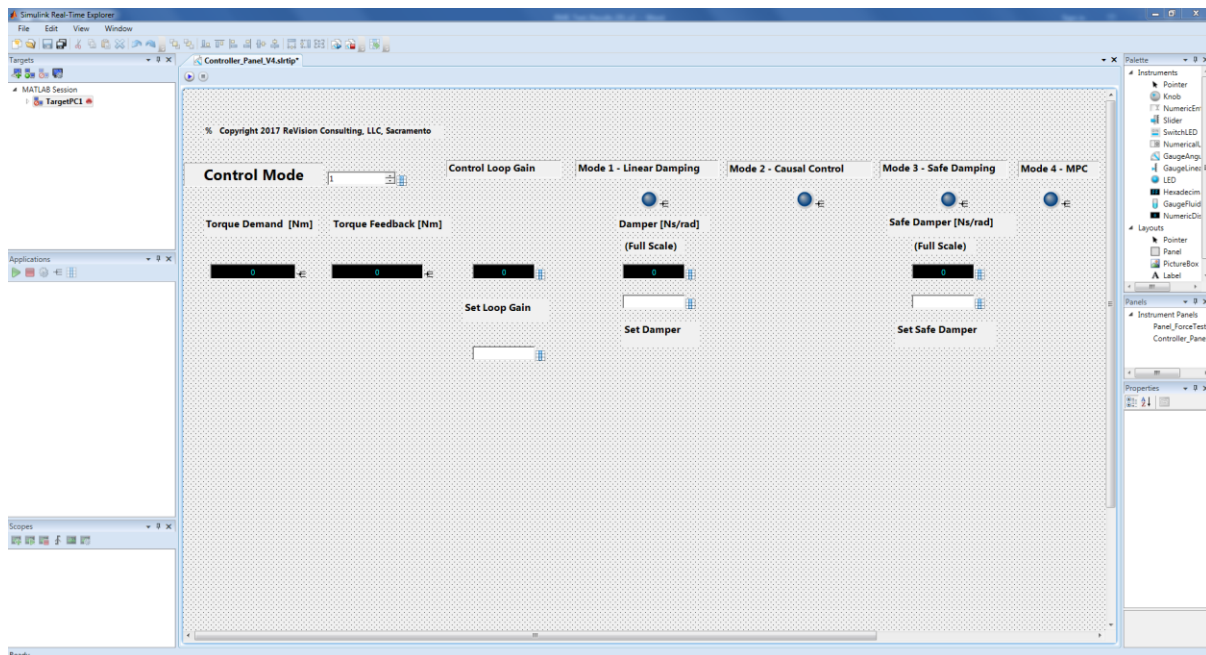


Figure 15. Front panel of real-time controller

7.3 CONTROL MODES

Three different control modes are considered in this work: Linear damping, Causal, and MPC. These control strategies are implemented on the real-time target machine, Speedgoat.

For linear damping control mode, the PTO is assumed to be linear damper system. This mode uses velocity feedback, and provide a force demand by multiplying linear damping value into the PTO. A damping value is constant and continuous value, which can be controlled on the front panel.

Causal control uses both position and velocity feedback signals, and provides a force demand signal into the PTO. Optimal tuning parameters needs to be set for different wave conditions.

MPC simply applies pre-determined PTO force-demand, which is optimized using an offline MPC optimization. For this purpose, wave information from wave gauge aligned with the device is needed in advance. In experiment, the optimized force time series is synchronized using the wave-maker trigger signal.

8 EXPERIMENTAL RESULTS AND VALIDATION

8.1 NOMENCLATURE

Table 12. Nomenclature of all variables and constant

	Symbol	Unit
Displaced mass	M	kg
Added mass	M_a	kg
Radiation damping	B	N/(m/s)
Viscous damping	B_{vis}	N/(m/s)
Total damping	$B_T=B+B_{vis}$	N/(m/s)
Hydrostatic stiffness	K_P	N/m
Damping ratio	ζ	-
Logarithmic decrement	δ	-
Damped natural period	T_d	sec
Damped natural frequency	ω_d	Rad/s
Natural frequency	ω_n	Rad/s
Wave number	k	m^{-1}
Water density	ρ	Kg/m^3
Drag coefficient	C_D	-
Water-plane area of the buoy	A	m^2
Wave amplitude	a	m
Group velocity	V_g	m/s
Wave-excitation force	F_{exc}	N

8.2 NUMERICAL RESULTS

The first step for determining hydrodynamic performance of the device is to obtain the hydrodynamic coefficients including; added mass M_a , radiation damping B , and wave-excitation force F_{exc} . The numerical hydrodynamic coefficients for given geometrical properties of the buoy in full scale were computed by WAMIT, which is plotted in Figure 16.

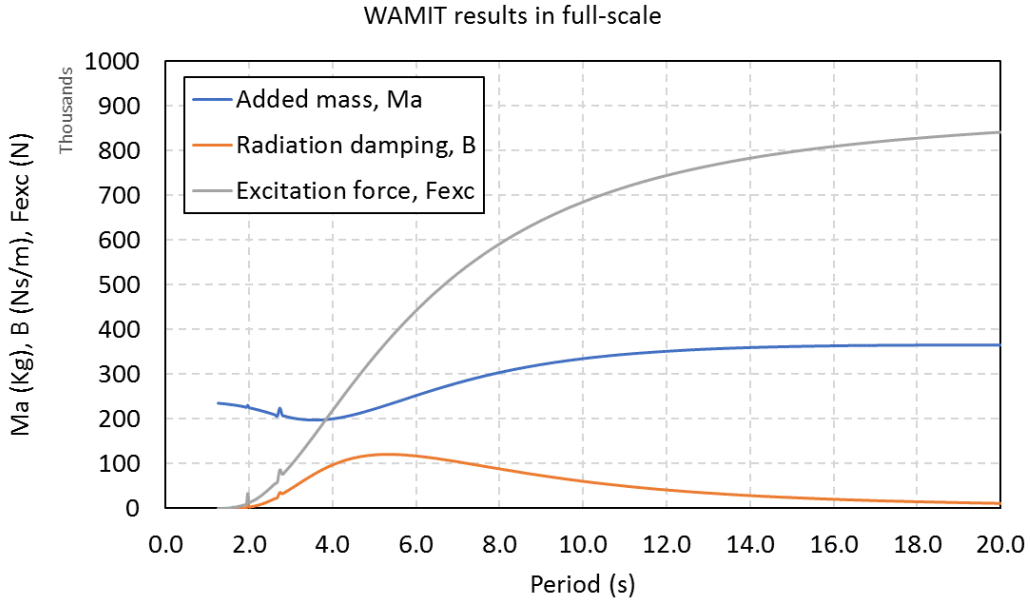


Figure 16. Hydrodynamic coefficients in model-scale from full-scale WAMIT analysis.

8.3 FREE-DECAY TEST

The oscillation of the buoy gradually decreases to its steady-state position after releasing from a certain initial displacement, which shows a typical underdamped mechanical system. The decaying period reveals the natural resonance frequency of the device using the logarithmic decrement method.

The damped mechanical system typically has the following form:

$$M\ddot{x} + B\dot{x} + K_p x = 0 \Rightarrow \ddot{x} + 2\zeta\omega_n\dot{x} + \omega_n^2 x = 0$$

where M , B and K_p are mass, damping and spring coefficient, respectively. Also, ζ and ω_n are the damping ratio and the natural frequency:

$$\zeta = \left(\frac{B}{M}\right)\left(\frac{1}{2\omega_n}\right)$$

$$\omega_n = \sqrt{\frac{K_p}{M}} = \frac{\omega_d}{\sqrt{1-\zeta^2}} = \frac{2\pi}{T_d\sqrt{1-\zeta^2}}$$

where ω_d represents the damped natural frequency.

In addition, the logarithmic decrement δ is obtained from the successive peaks and related to the damping ratio:

$$\delta = \ln\left(\frac{y_n}{y_{n+1}}\right) = \zeta\omega_n T_d = \zeta\omega_n \frac{2\pi}{\omega_d} = \frac{2\pi\zeta}{(1-\zeta^2)}, \text{ or } \zeta = \frac{\delta}{\sqrt{4\pi^2 + \delta^2}}$$

Thus, the natural frequency is obtained from the oscillation data of the device over time as shown in Figure 17. With the use of the added mass coefficients from WAMIT, the spring stiffness and damping value considering a linear-viscous damping term in real fluid were deduced:

$$\omega_n = \sqrt{K_p / (M + M_a)} \Rightarrow K_p = \omega_n^2 (M + M_a)$$

$$B_T = B + B_{vis} = 2\zeta\omega_n (M + M_a)$$

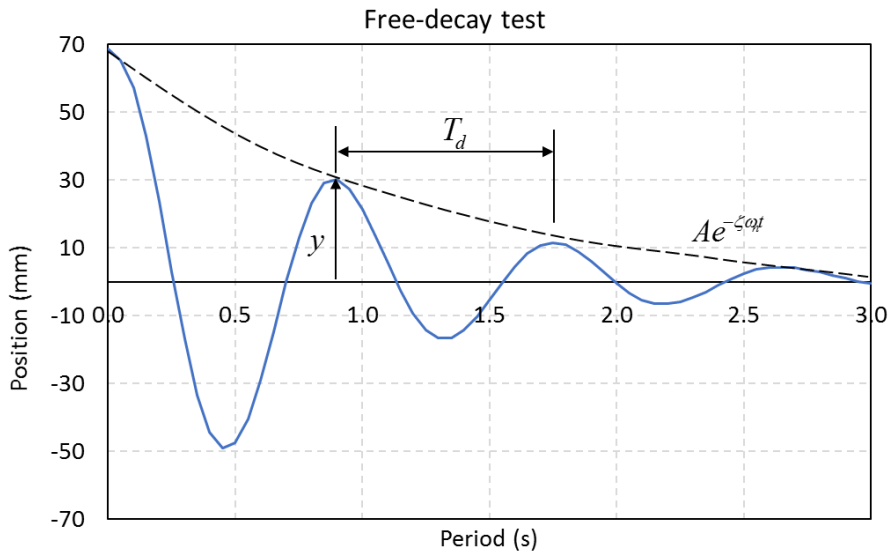


Figure 17. Time history of the buoy position after initial position

A summary of the free-decay test results is listed in Table 13. Initially, a linear drag or viscous damping value was assumed as follows:

$$B_{vis} = 0.5 \times C_D \times \rho \times A$$

where $C_D = 0.5$, $\rho = 1025 \text{ kg/m}^3$, and A is the water-plane area.

It turns out that the measured resonance frequency matches well with prediction, and measured linear viscous damping value is close to the prediction.

Table 13. Summary of free-decay test results

	Full-scale (WAMIT)	Model-scale (WAMIT)	Model-scale (Experiment)
Natural resonance period (s)	4.5	0.9	0.88
Natural resonance frequency (rad/s)	1.40	7.0	7.17
Displaced mass, M (kg)	233781.62	14.96	14.96
Added mass at resonance freq., M_a (kg)	210100	13.45	
Hydrostatic restoring stiffness, K_p (N/m)	899275.7	1438.8	1460.1
Radiation damping at resonance freq., B (N/(m/s))	111801.5	35.78	
Total damping including viscous effects, $B_T=B+B_{vis}$	-	-	47.97
Linear-viscous damping, B_{vis}	24352.25	7.79	12.19

8.4 WAVE-EXCITATION FORCE

With a fixed position of the buoy, measured wave-excitation force was measured and compared to the WAMIT results as a function of incident-wave period in full scale, which is shown in Figure 18. Measurements match well with predictions.

The Haskind's relation represents reciprocity relation between wave-excitation force and damping:

$$F_{exc} = a \left[\frac{4\rho g V_g}{k} B \right]^{1/2}$$

where a is the incident-wave amplitude, V_g is the group velocity, k is the wave number, and B is the radiation damping.

The computed wave-excitation force from the Haskind's relation has the same results with numerical results. Thus, it proves that the radiation damping between the prediction and the experiment agrees well.

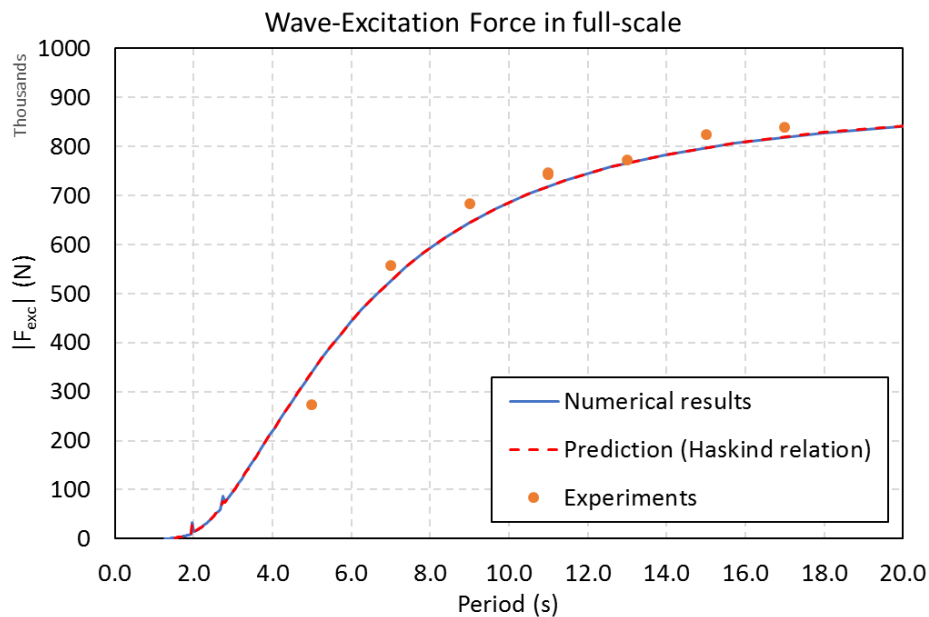


Figure 18. Wave-excitation force comparison

8.5 POWER PERFORMANCE IN REGULAR WAVES

8.5.1 PTO force control

Reaction force of the PTO affects the motion response of the buoy to incident waves as well as power extraction. Thus, the PTO force was controlled during the test to investigate the motion response and power extraction performance. With use of the permanent magnet linear motor as the PTO, internal PI algorithm of LinMot drive was used for the force control loop. The purpose of the force control loop is to match actual force to desired force demand. PI gains are adjustable on the motor drive, and set to $P=0.1$ and $I=2$ for experiments. A schematic of the PTO force control loop is illustrated in Figure 19.

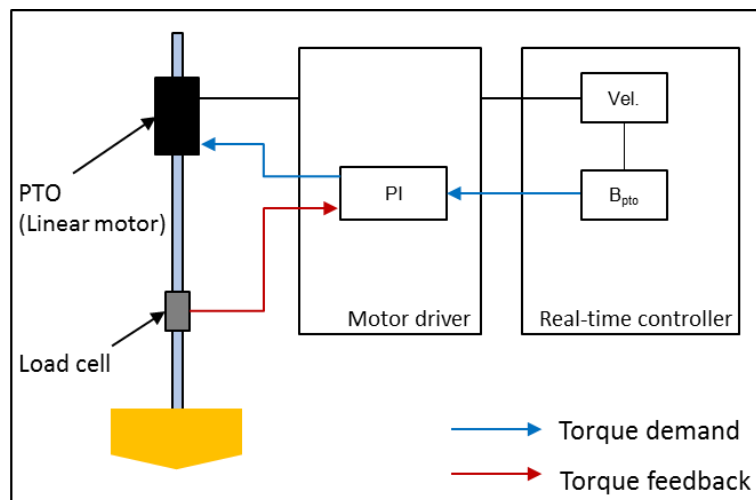


Figure 19. Schematic of PTO control loop

8.5.2 Power extraction performance results

A) TEST CAMPAIGN I

During Test Campaign I, a few performance tests performed to verify operation of the device in different control modes. In testing with linear damping control mode, two things were observed: (1) increasing motion response with increasing PTO damping shown in Figure 20; (2) time delay in force feedback from force input shown in Figure 21.

It is expected that motion response decreases with increasing PTO damping because PTO force applies against motion velocity. It turns out that force input direction of the PTO was wrong during the testing, thus feeding power into waves not extracting power from waves. The time delay between force input to the PTO and feedback from load cell was also observed in MPC mode trials, which can be found in Figure 22, as an example of $T = 11$ sec (2.2 sec in model scale). In addition, measured motion response and absorbed power lag simulation results when compared in time domain as shown in Figure 23 to Figure 25. However, experimental results have a similar amplitude with simulation results, so measured time-averaged power extraction agrees with simulation as shown in Figure 26. The time delay issue on feedback signal was resolved by updating IO module driver of the Speedgoat after Test Campaign I was complete.

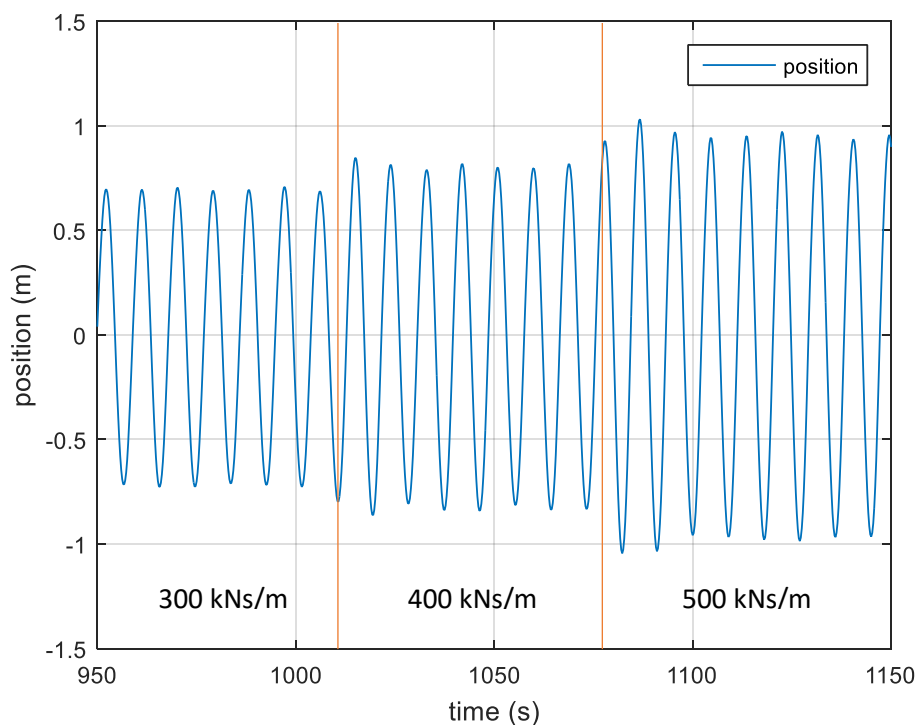


Figure 20. Time history of motion response with different linear damping values – Test Campaign I

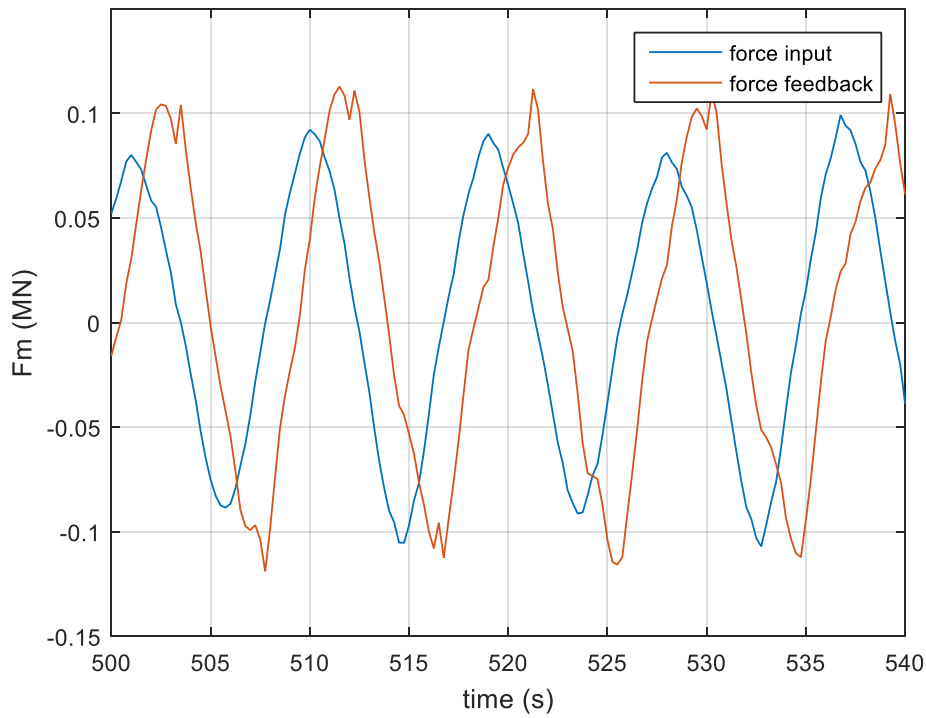


Figure 21. Time history of PTO force between input and feedback with linear damping – Test Campaign I

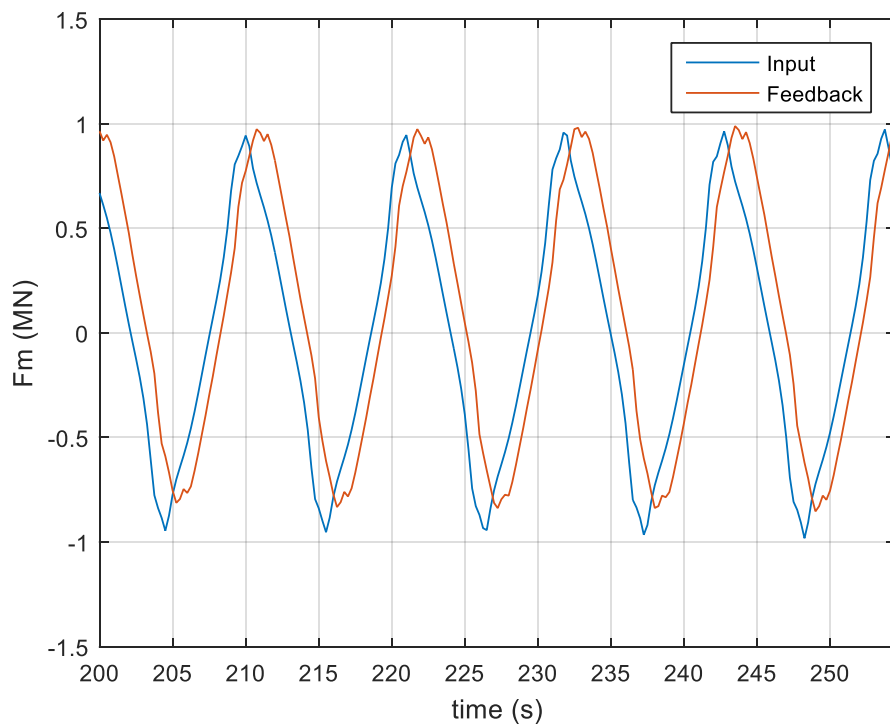


Figure 22. Time history of PTO force between input and feedback with MPC– Test Campaign I

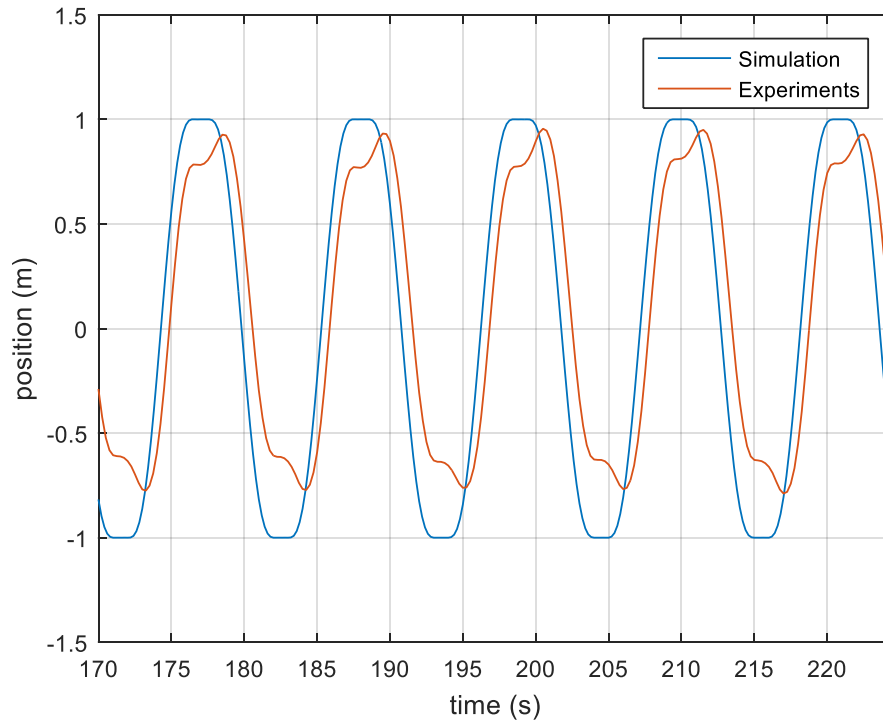


Figure 23. Time history of displacement between simulation and measurement with MPC- Test Campaign I

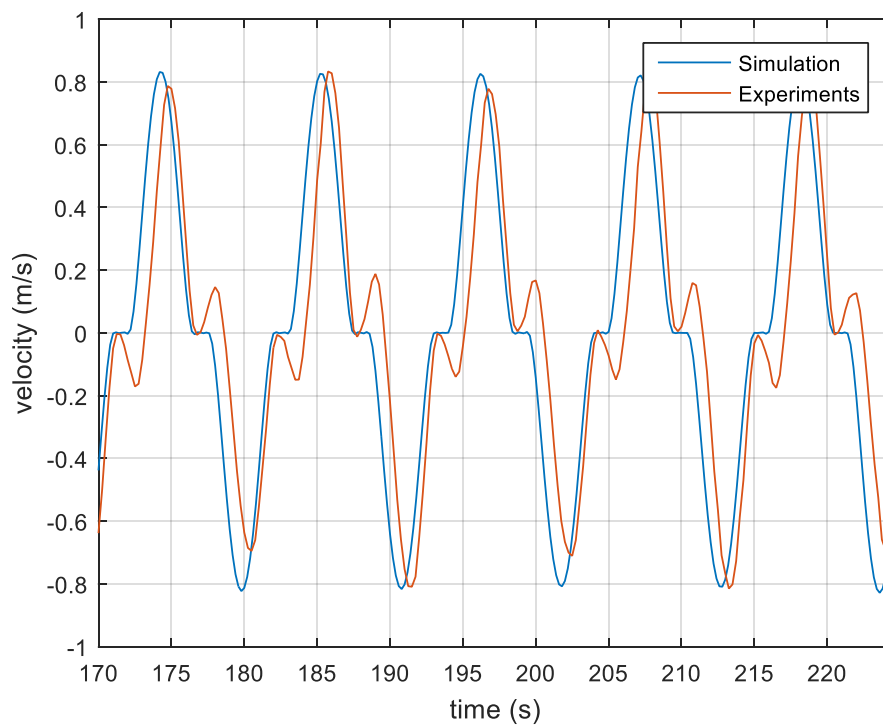


Figure 24. Time history of velocity between simulation and measurement with MPC – Test Campaign I

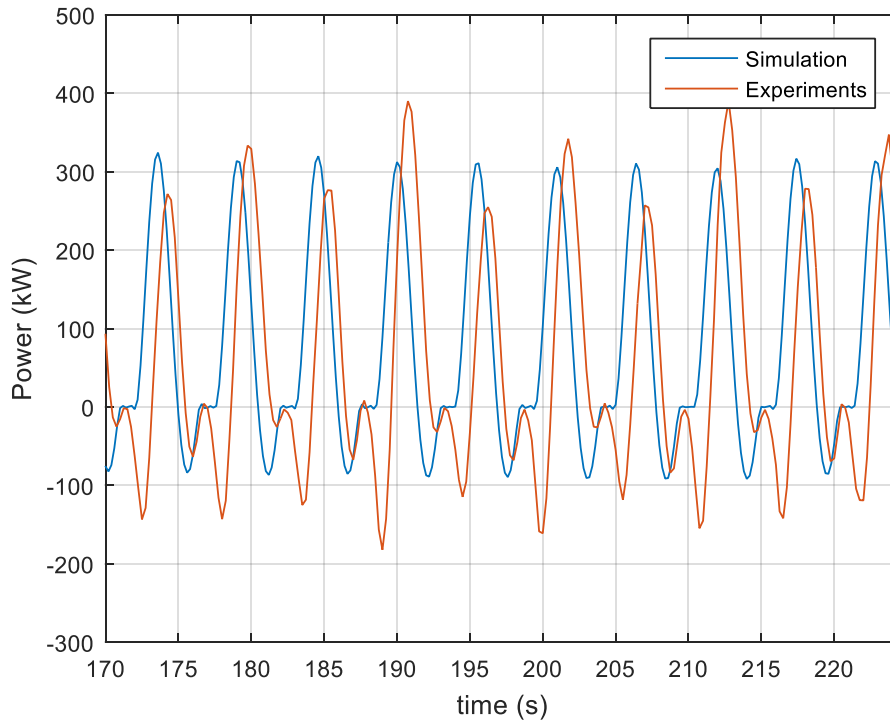


Figure 25. Time history of absorbed power between simulation and measurement with MPC – Test Campaign I

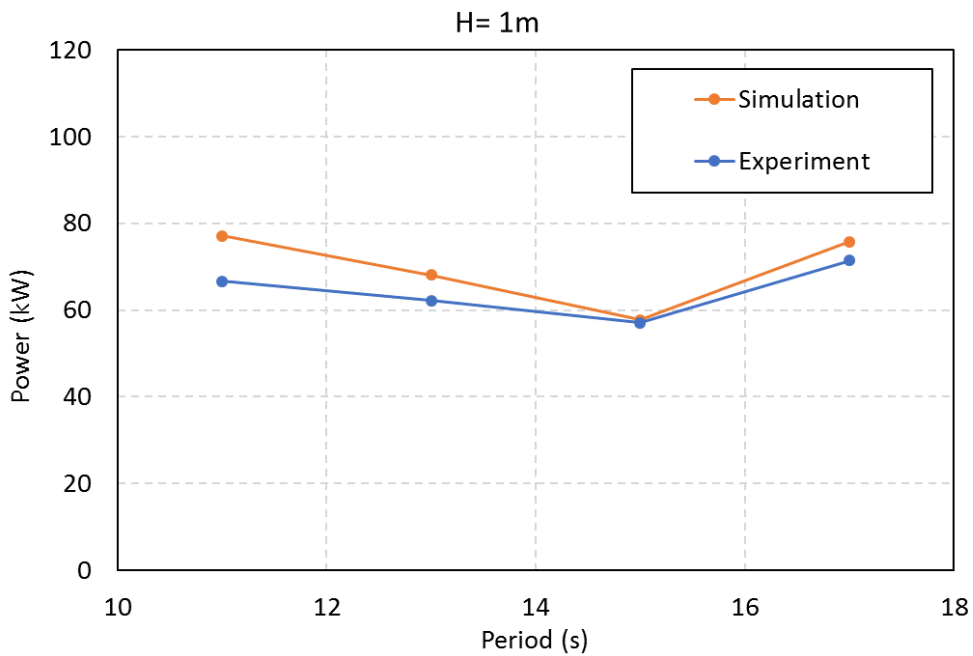


Figure 26. Time-averaged power performance with MPC – Test Campaign I

B) TEST CAMPAIGN II

By fixing the force input direction of the PTO and updating the hardware driver of the target machine, the issues observed in Test Campaign I disappeared. The heave response amplitude of operator (RAO), amplitude of motion response with respect to amplitude of incident wave, decreases with increasing PTO damping value, as shown in Figure 27. The phase shift between force input to PTO and feedback from load cell is significantly reduced and is negligible, which is shown in Figure 28.

Each frequency has a different optimal PTO damping at which maximum power is captured. By sweeping different PTO damping values for given frequencies, an optimal linear damping was found as shown in Figure 29. As an example of $T = 9$ sec, Figure 30 shows instantaneous power, applied PTO force, and motion responses with the optimal damping value of 1200 kN/(m/s) in time domain. In addition, time histories of performance for causal control and MPC are plotted in Figure 31 and Figure 32.

As a summary of this Test Campaign II, time-averaged power absorption for 1m incident-wave height as a function of frequency with different control methods is plotted in Figure 33. Obviously, the causal control and MPC improve performance of the power capture when compared to the constant linear damping control. For the simulation results, an actual wave data measured from wave gauge was used not to overestimate performance with ideal sinusoidal waves. Overall trends between experiment and simulation agree for all control modes, but fine tuning of developed numerical model is needed for better matching with experimental results.

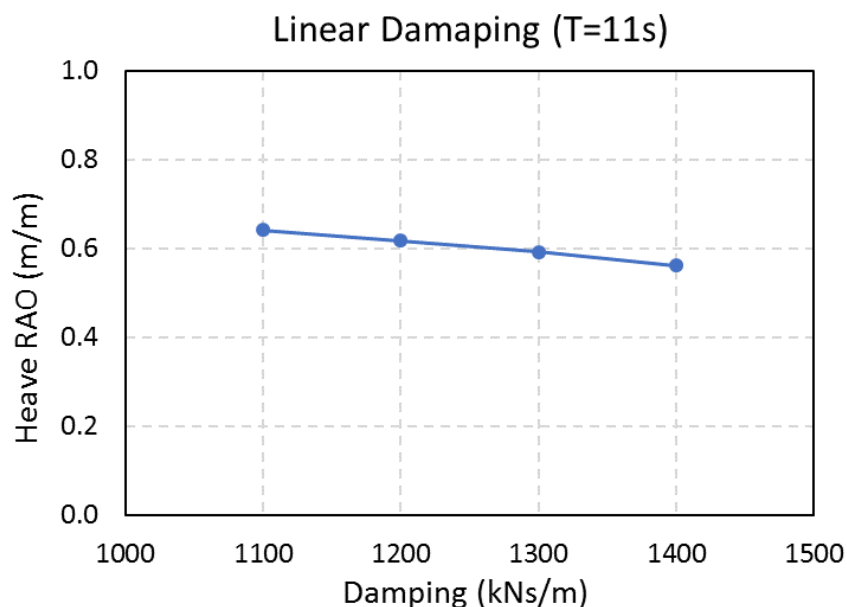


Figure 27. Heave response amplitude of operator for different linear damping - Test Campaign II

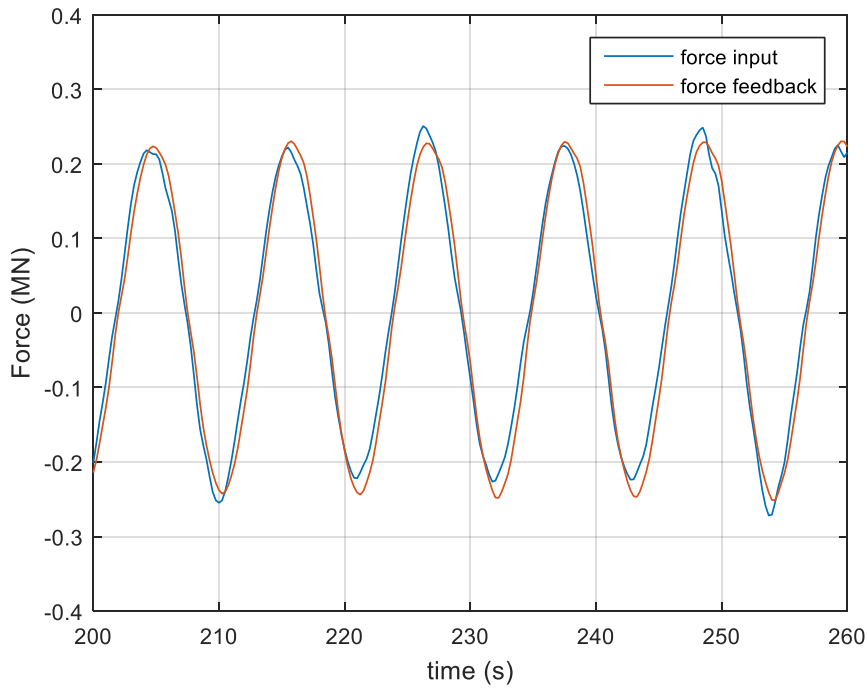


Figure 28. Time history of PTO force between input and feedback with linear damping - Test Campaign II

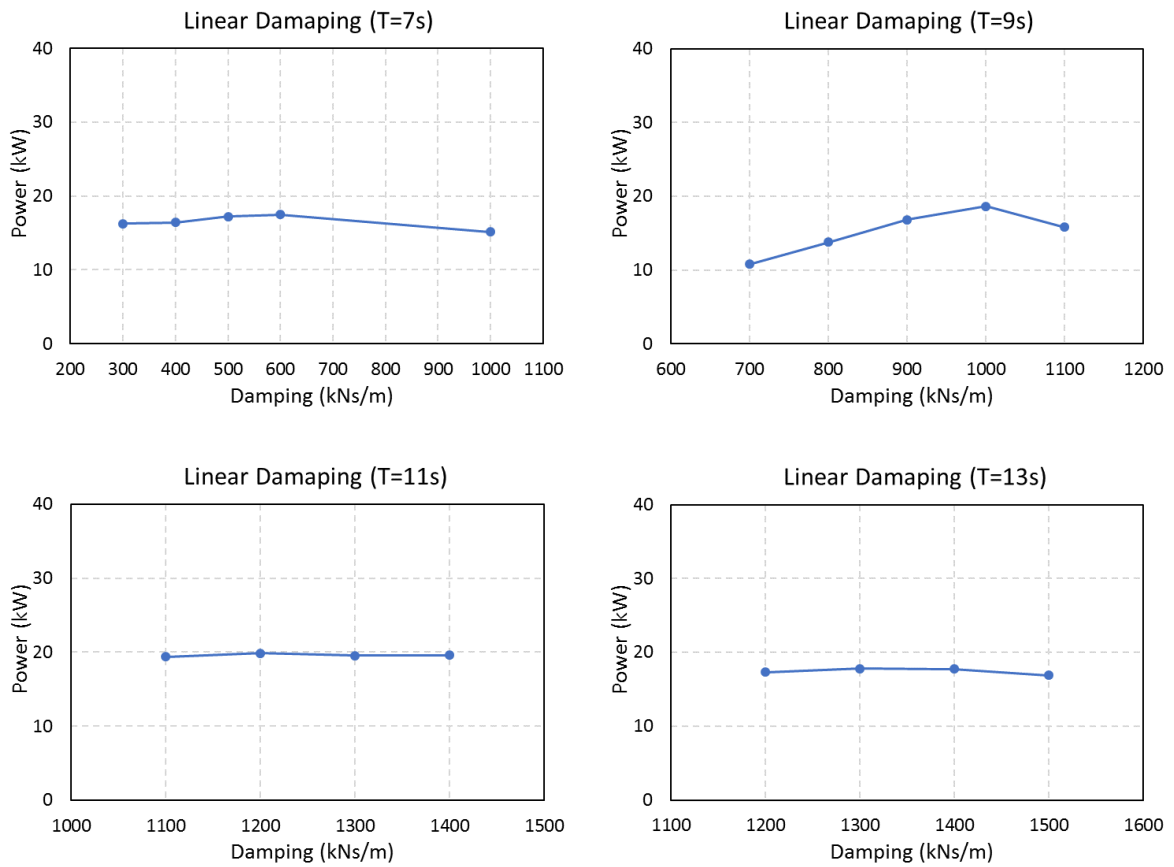


Figure 29. Linear damping optimization - Test Campaign II

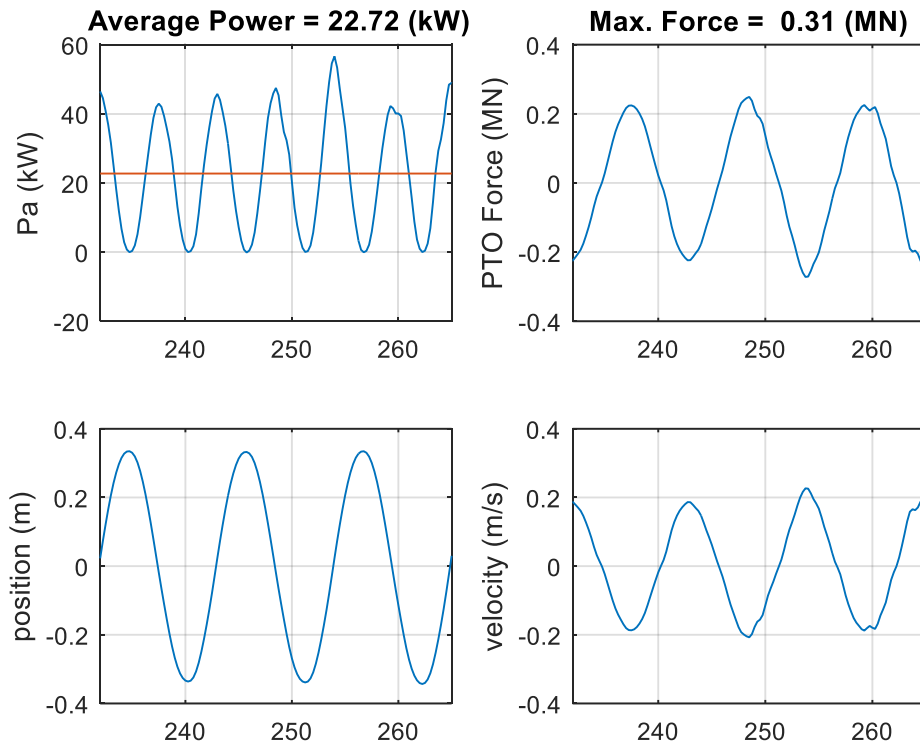


Figure 30. Performance with linear damping in time series - Test Campaign II

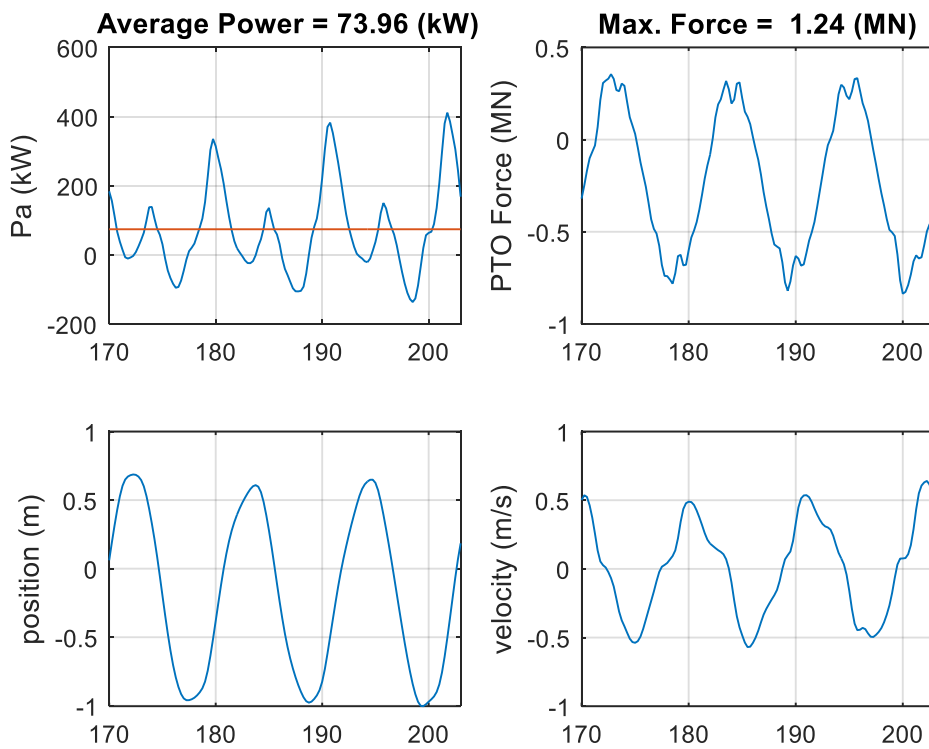


Figure 31. Performance with causal control in time series - Test Campaign II

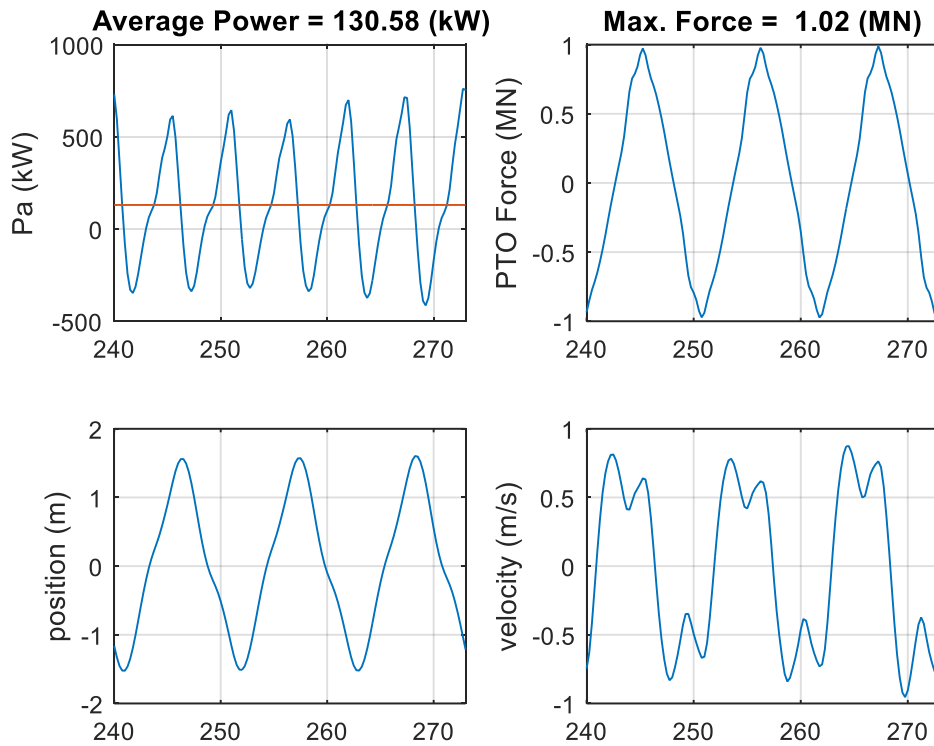


Figure 32. Performance with MPC in time series - Test Campaign II

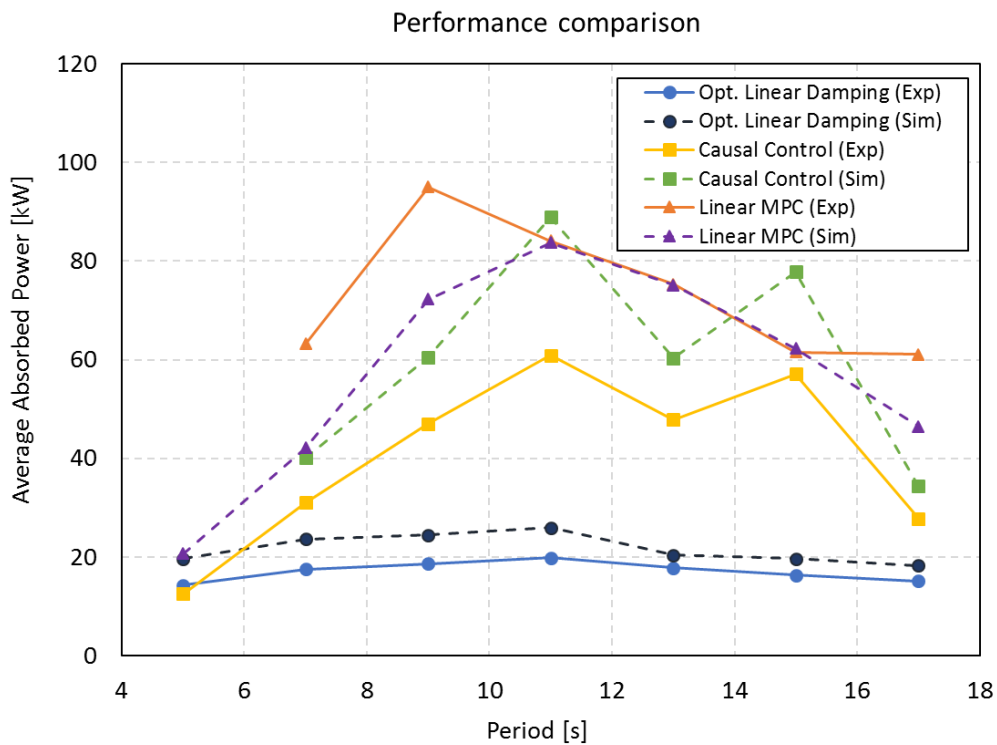


Figure 33. Time-averaged power performance - Test Campaign II

C) TEST CAMPAIGN III

The Test Campaign III repeated previous test matrix, but with tuned numerical model parameters, to verify the performance improvement by causal control and MPC than that of linear damping control. Figure 34 shows searching of the optimal damping at each frequency, and compares with predicted power computed by simulation. A found optimal linear damping from experimental results has the same with one from simulation results as well as time-averaged power value. Absorbed power, PTO force, and motion responses in time domain for three different control methods are plotted in Figure 36 to Figure 38, which is at 11 sec wave periods. For the MPC, measurements and simulation results for selected periods are compared through Figure 39 to Figure 42. It shows good agreement between them, even in latching-like velocity behavior.

Figure 43 presents time-averaged power as a function of frequency. At a glance, causal control and MPC improve performance in power extraction, especially 9 sec wave periods onward. The causal control and MPC lead to maximum 3-fold and 5-fold power performance respectively when compared to the optimal linear damping control. Figure 44 is the heave response amplitude of operator (RAO) in the same way with power comparison. It is consistent with power performance results, and can explain power improvement by the causal control and MPC.

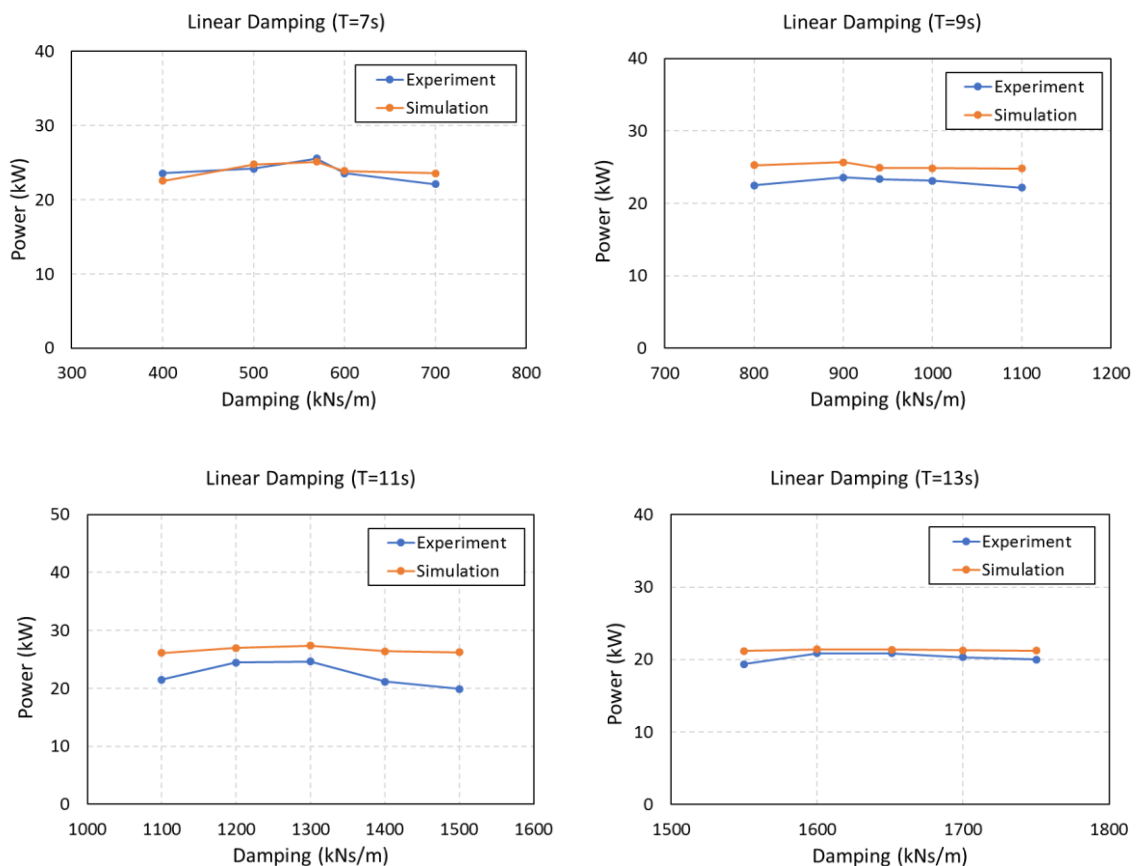


Figure 34. Linear damping optimization - Test Campaign III

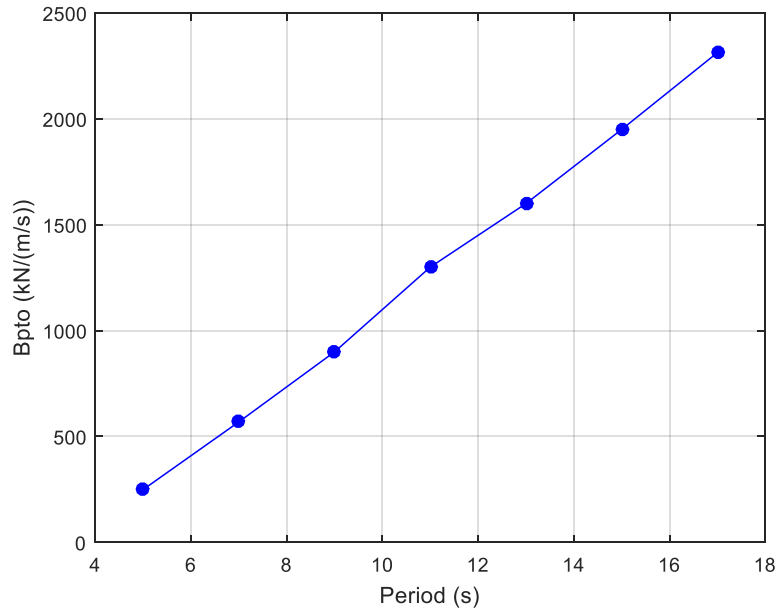


Figure 35. Optimal linear damping for each wave period

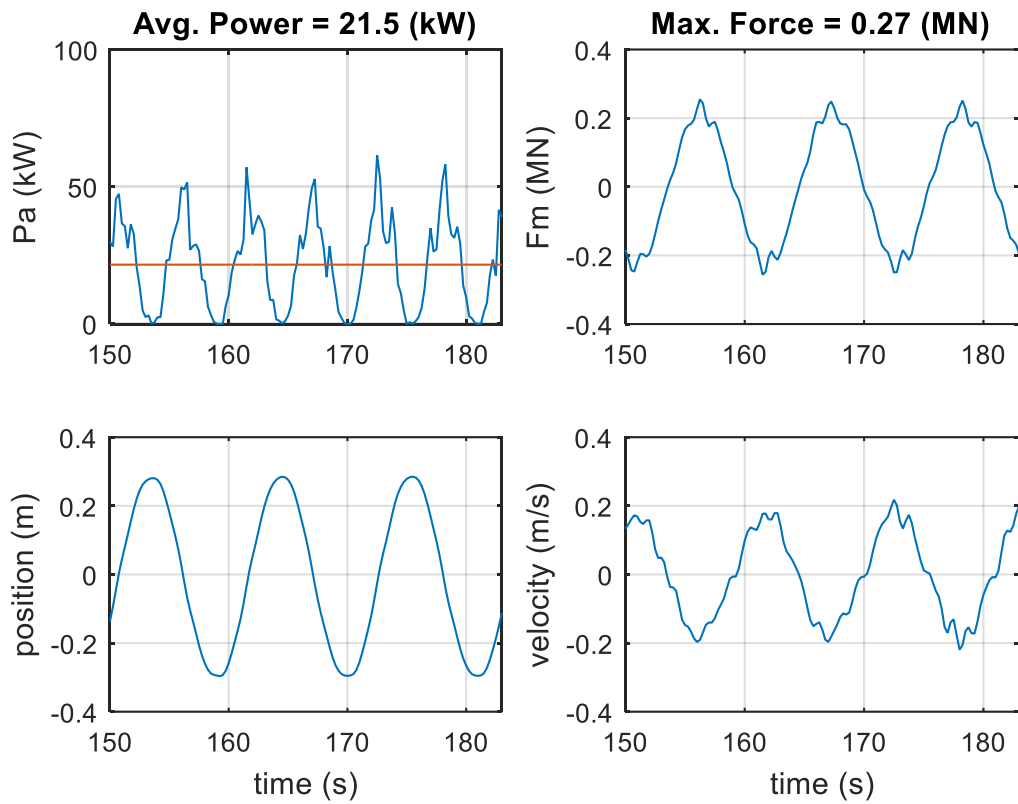


Figure 36. Performance for linear damping in time series - Test Campaign III

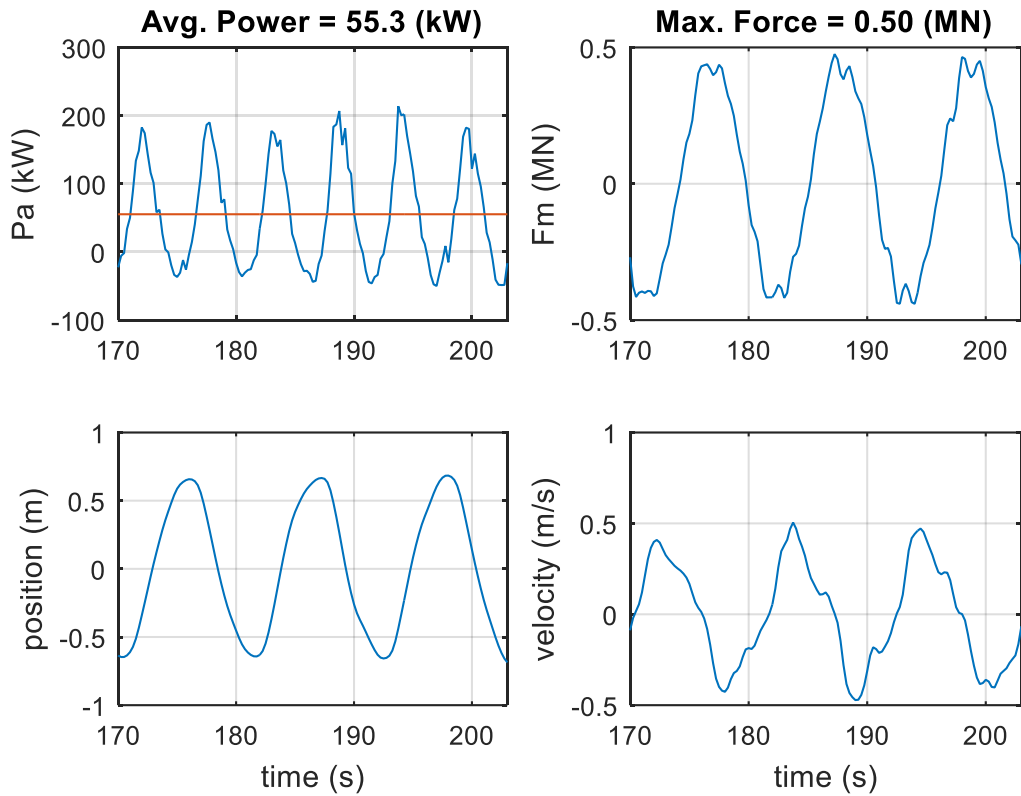


Figure 37. Performance for causal control in time series - Test Campaign III

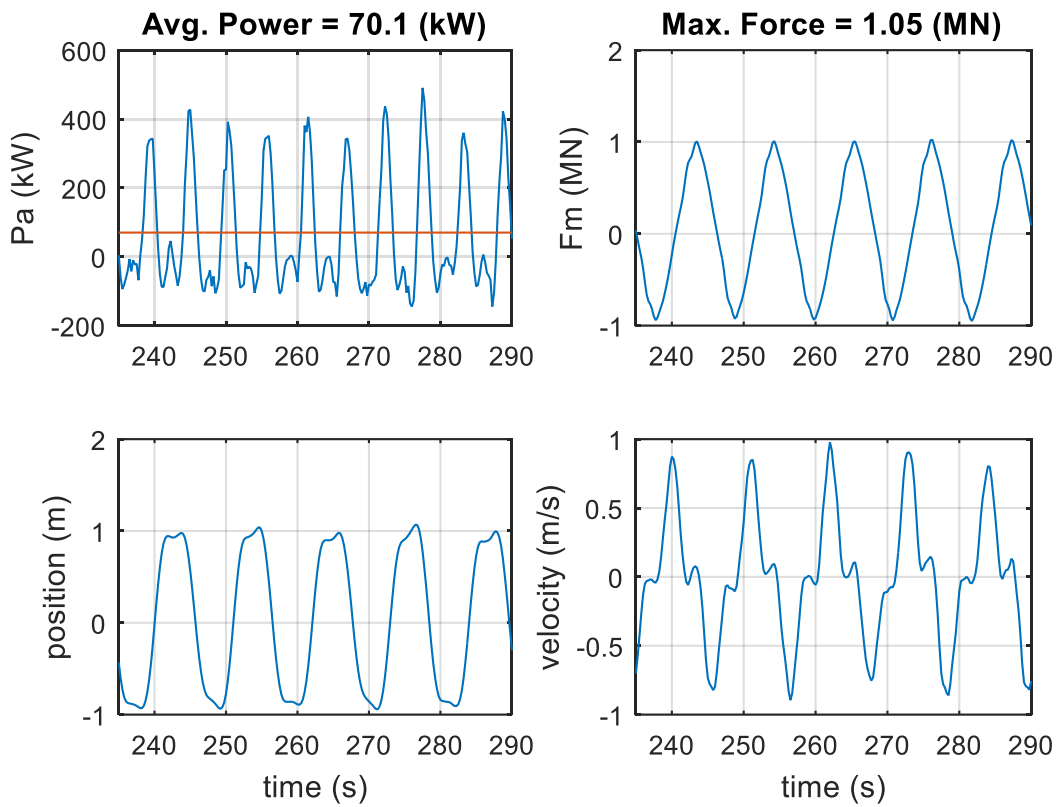


Figure 38. Performance for linear MPC in time series - Test Campaign III

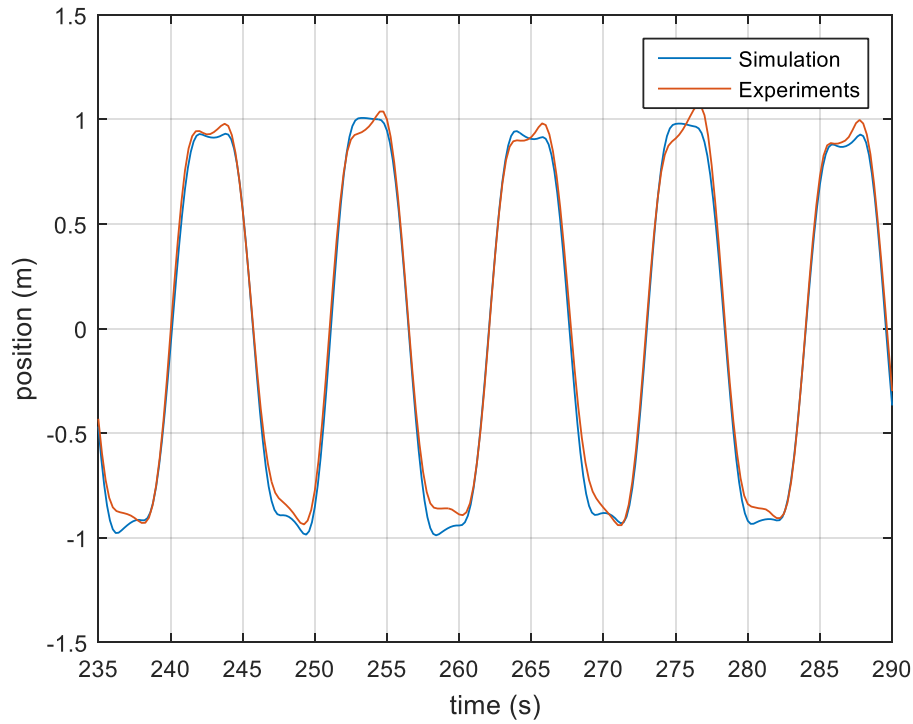


Figure 39. Position comparison between simulation and experiment with MPC – Test Campaign III

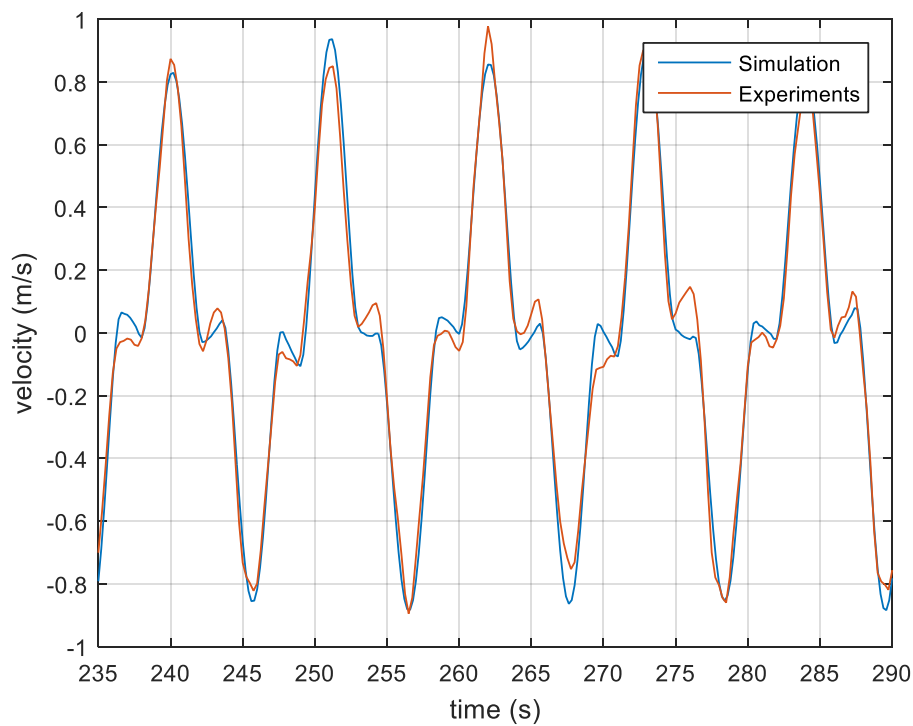


Figure 40. Velocity comparison between simulation and experiment with MPC - Test Campaign III

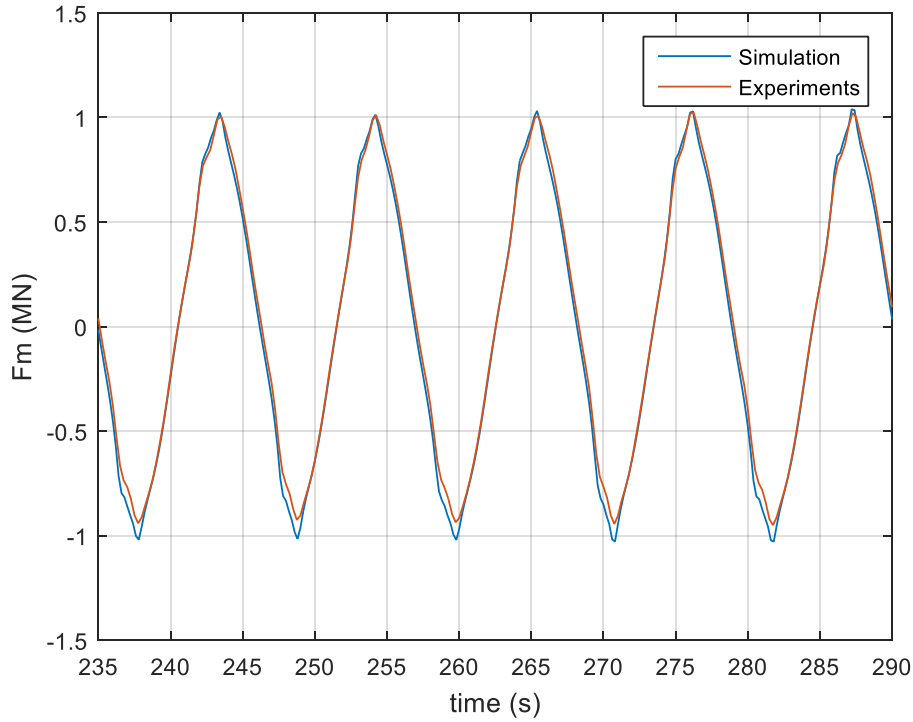


Figure 41. PTO force comparison between simulation and experiment with MPC - Test Campaign III

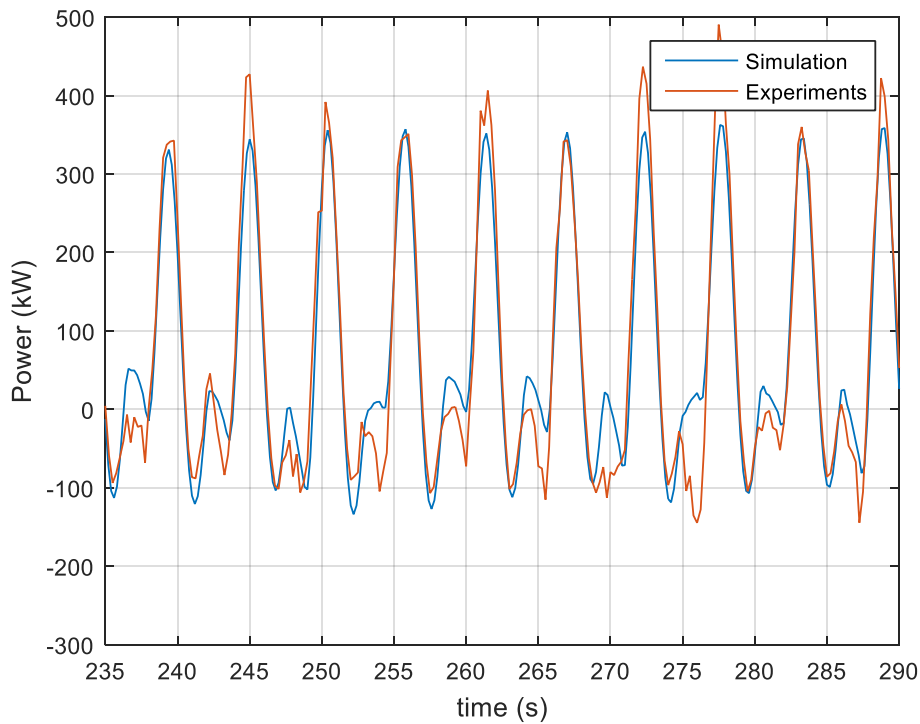


Figure 42. Power comparison between simulation and experiment with MPC - Test Campaign III

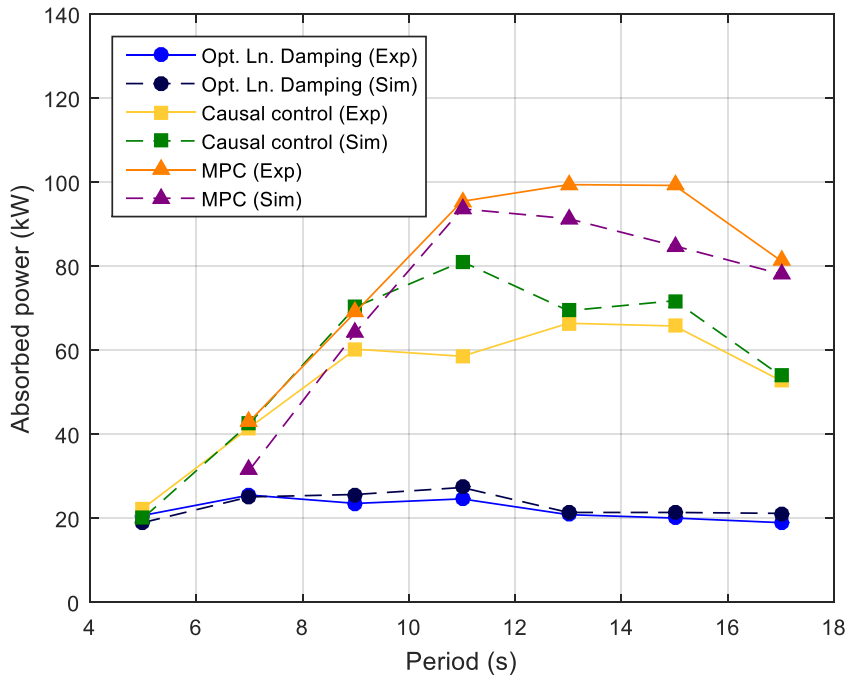


Figure 43. Time-averaged power performance - Test Campaign III

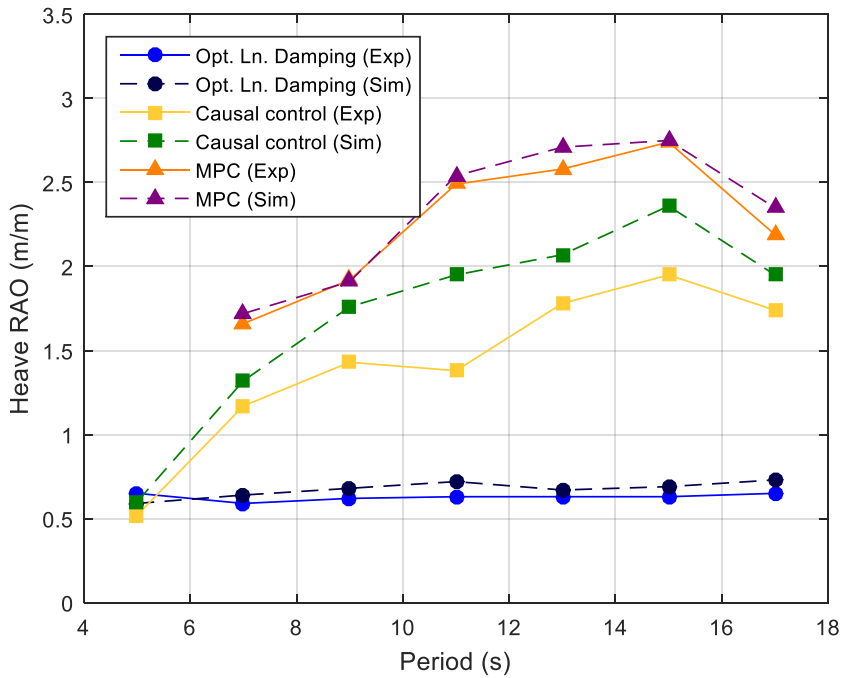


Figure 44. Heave response amplitude of operator - Test Campaign III

In order to confirm the power performance improvement brought by the MPC, tests were also performed in irregular waves. For this purpose, a JONSWAP spectrum with significant wave height of 1m and peak period of 11s in full scale was used. An optimal damping of 1013600 Ns/m was found from simulation study for linear damping control, and performance for certain time window is plotted in Figure 45. In the same way, performance controlled by MPC can be found in Figure 46. Those results indicate the MPC significantly improves absorbed power by factor of about 4; measured mean power absorption for [100s, 2500s] is about 10kW by linear damping control and 38kW by MPC.

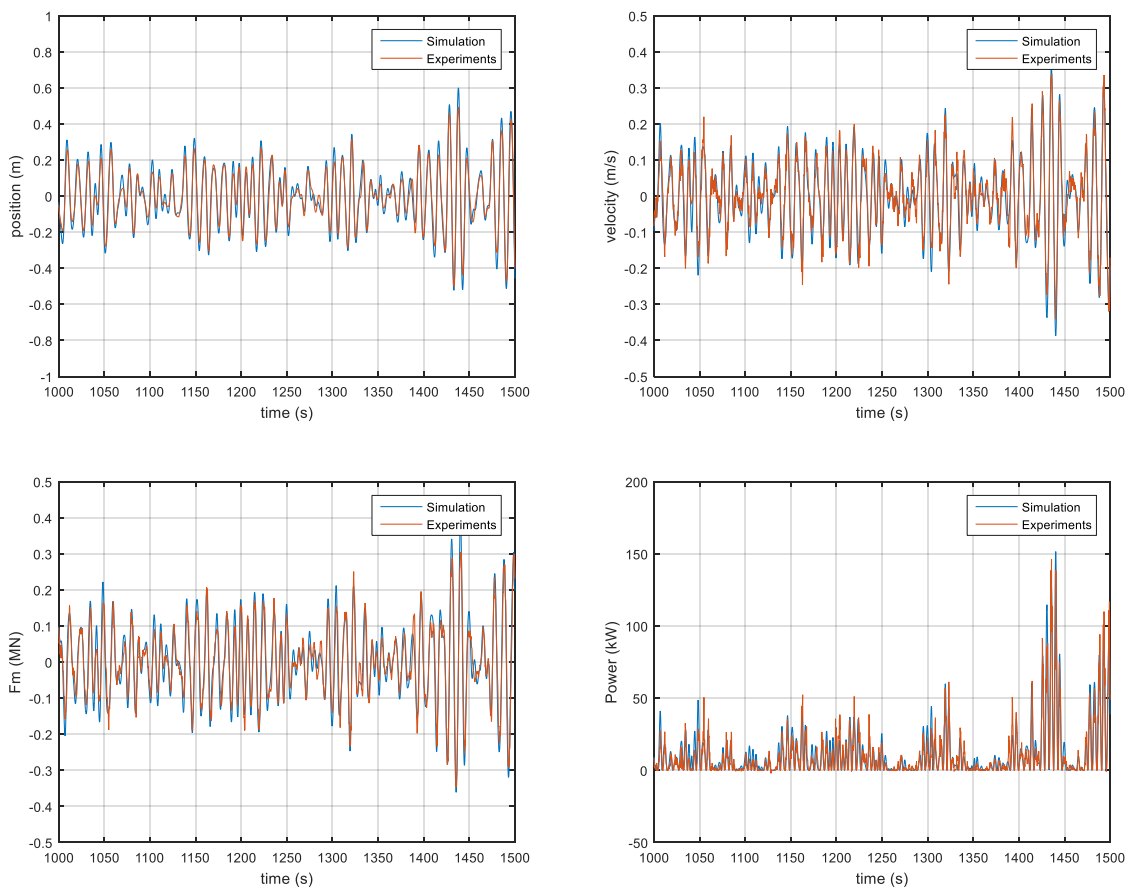


Figure 45. Performance with optimal linear damping in irregular waves

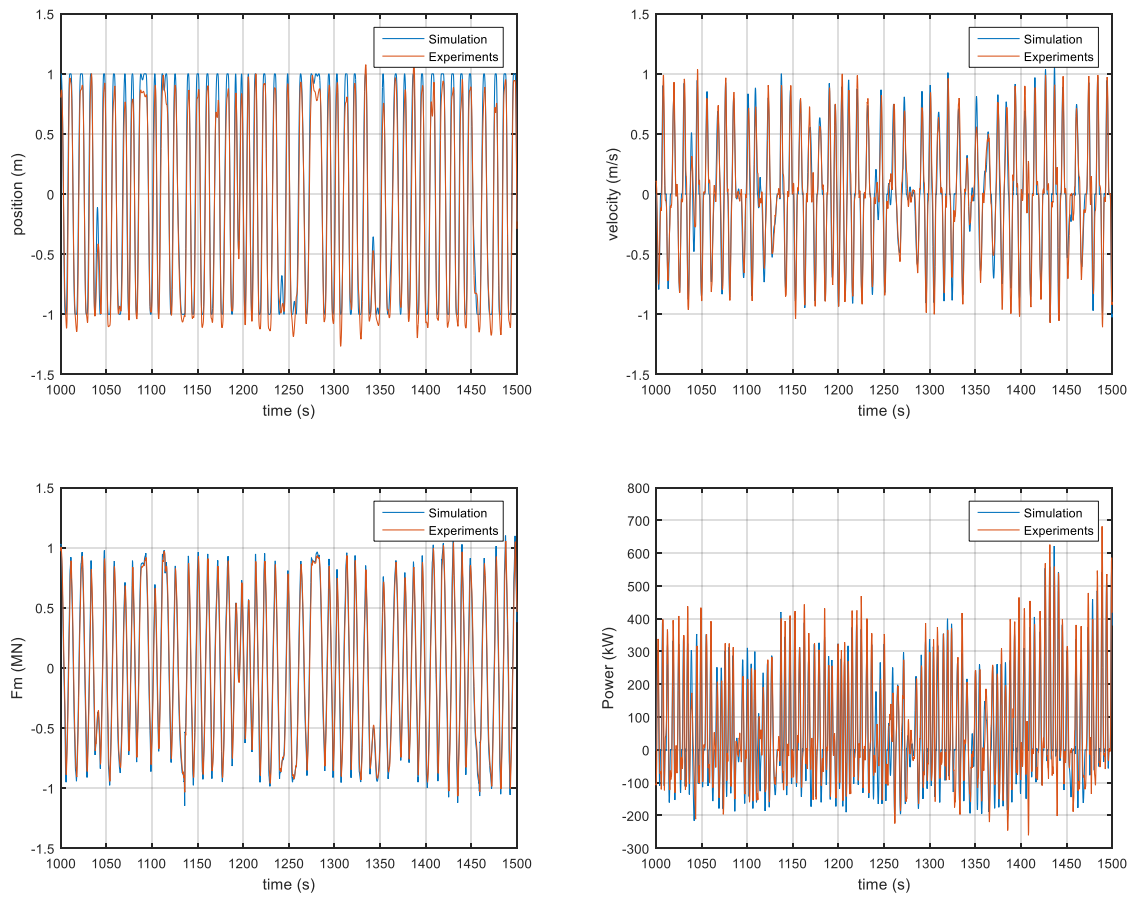


Figure 46. Performance with MPC in irregular waves

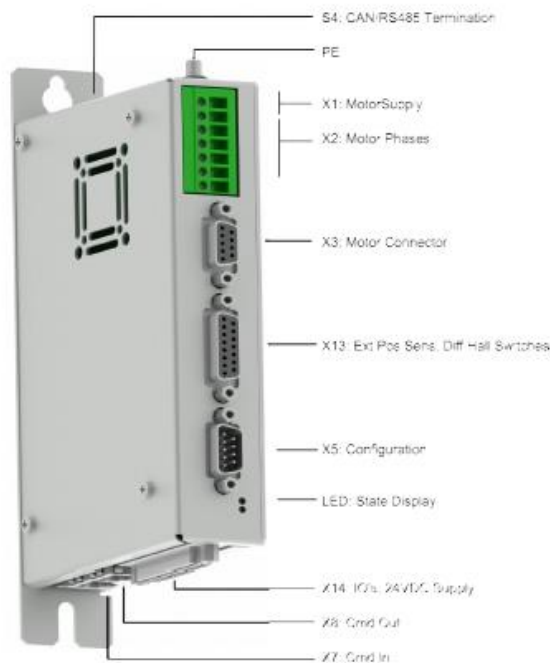
APPENDIX A: SPECIFICATIONS – MOTOR

1. PS01-37x120C

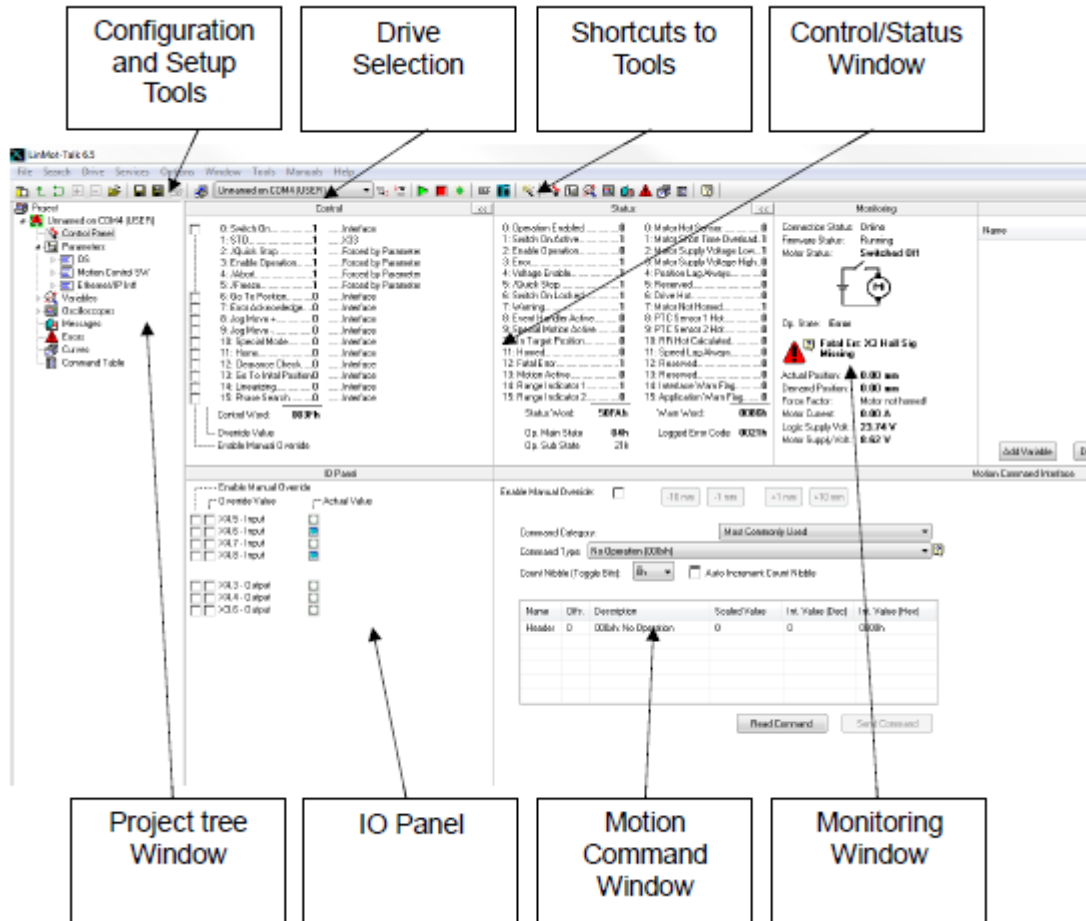
Motor Specification

	P01-	Connector Type	Cable Type
		37x120/1380x1460-C	37x120/1380x1460-P150 37x120/1380x1460-C20
Extended Stroke ES	mm (in)	1460 (57.48)	1460 (57.48)
Standard Stroke SS	mm (in)	1380 (54.33)	1380 (54.33)
Peak Force E1100-HC	N (lbf)	163 (36.7)	163 (36.7)
Peak Force E1100 / E1001	N (lbf)	163 (36.7)	163 (36.7)
Cont. Force	N (lbf)	29 (6.5)	29 (6.5)
Cont. Force Fan cooling	N (lbf)	54 (12.2)	54 (12.2)
Border Force	%	67	67
Force Constant	N/A (lbf/A)	20.4 (4.59)	20.4 (4.59)
Max. Current @ 72VDC	A	8.0	8.0
Max. Current @ 48VDC	A	6.3	6.3
Max. Velocity @ 72VDC	m/s (in/s)	3.2 (128)	3.2 (128)
Max. Velocity @ 48VDC	m/s (in/s)	2.2 (85)	2.2 (85)
Phase Resist. 25/80 °C	Ohm	6.2/7.5	6.2/7.5
Phase Inductance	mH	3.1	3.1
Thermal Resistance	°K/W	3.6	3.6
Thermal Time Const.	sec	2900	2900
Stator Diameter	mm (in)	37 (1.46)	37 (1.46)
Stator Length	mm (in)	216 (8.50)	227 (8.94)
Stator Mass	g (lb)	740 (1.63)	740 (1.63)
Slider Diameter	mm (in)	20 (0.79)	20 (0.79)
Slider Length	mm (in)	1600 (62.99)	1600 (62.99)
Slider Mass	g (lb)	3622 (7.99)	3622 (7.99)
Position Repeatability	mm (in)	±0.05 (±0.0020)	±0.05 (±0.0020)
Linearity	%	±0.10	±0.10
Repeatability with EPS	mm (in)	±0.01 (±0.0004)	±0.01 (±0.0004)
Linearity with EPS	mm (in)	±0.01 (±0.0004)	±0.01 (±0.0004)

2. B1100-GP drive



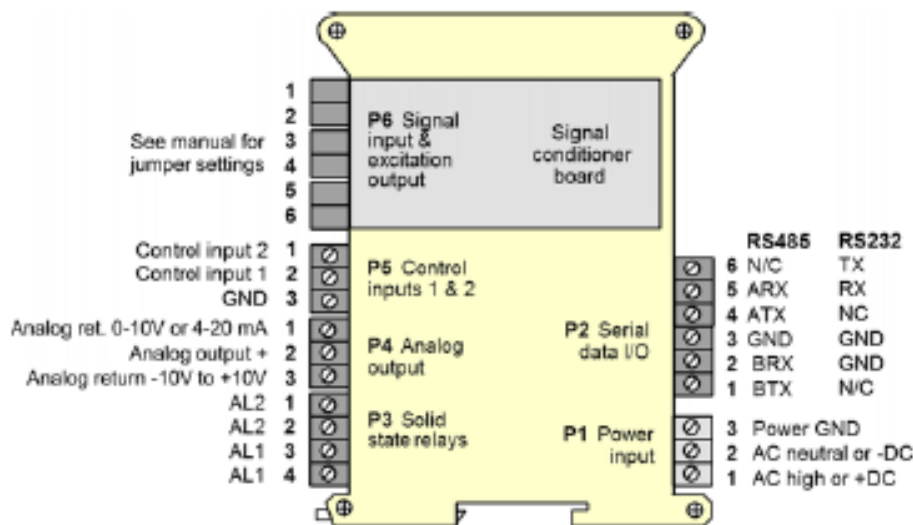
3. LinMot-Talk



The screenshot shows the LinMot-Talk 6.5 software interface. Callouts identify the following windows:

- Configuration and Setup Tools**: Points to the top-left menu area.
- Drive Selection**: Points to the 'Control' pane on the left.
- Shortcuts to Tools**: Points to the top toolbar.
- Control/Status Window**: Points to the 'Status' pane on the right.
- Project tree Window**: Points to the left sidebar.
- IO Panel**: Points to the 'IO Panel' section in the center.
- Motion Command Window**: Points to the 'Motion Command' section in the center.
- Monitoring Window**: Points to the 'Monitoring' section on the right.

4. Pinout for position measurement – LT61QD



APPENDIX B: SPECIFICATIONS – SENSOR

1. LSB200 load cell (S/N 660406)

SPECIFICATIONS	
PERFORMANCE	
Nonlinearity	±0.1% of RO
Hysteresis	±0.1% of RO
Nonrepeatability	±0.05% of RO
ELECTRICAL	
Rated Output (RO)	See chart on third page
Excitation (VDC or VAC)	10 max
Bridge Resistance	See chart on third page
Insulation Resistance	≥500 MOhm @ 50 VDC
Connection	#29 AWG, 4 conductor, spiral shielded silicone cable, 5 ft [1.5 m] long
Wiring/Connector Code	WC1
MECHANICAL	
Weight (approximate)	0.3 oz [9 g]
Safe Overload	1000% of RO 200% tension only (50–100 lb)
Material	Aluminum (10 g–10 lb), stainless-steel (25–100 lb)
IP Rating	IP40
TEMPERATURE	
Operating Temperature	-60 to 200°F [-50 to 93°C]
Compensated Temperature	60 to 160°F [15 to 72°C]
Temperature Shift Zero	±0.01% of RO/°F [0.018% of RO/°C]
Temperature Shift Span	±0.02% of Load/°F [0.036% of Load/°C]
CALIBRATION	
Calibration Test Excitation	5 VDC
Calibration (standard)	5-pt Tension
Calibration (available)	Compression

2. Wiring color code

WIRING CODE (WC1)	
RED	+ EXCITATION
BLACK	- EXCITATION
GREEN	+ SIGNAL
WHITE	- SIGNAL
SHIELD	FLOATING

APPENDIX C: SPECIFICATIONS —SPEEDGOAT

1. Real-time target machine

Housing	
Enclosure	4U 19"-compatible aluminium chassis / I/O front-accessible (standard) I/O front or rear accessible (deep option)
Color	Silver powder-coated, natural aluminium
External dimensions	Height: 177.8mm (4U) Width: 440mm, 480mm (including rack mounts) Depth (standard): 360mm (400mm including handles) Depth (deep option): 440mm (480mm including handles)
Weight	12kg (excluding I/O modules, cables, and terminal boards)
Power supply	400W, 100-240V, 50-60Hz, fan-less, zero-noise
Fans	Two at rear (outtake), high quality, low-noise Papst fans
Handles	2 for desktop use 2 for rack installation
Certification	CE and FCC certified
Mainboard & CPU	
Processor	Intel Core i3 3.3GHz (standard) Intel Core i7 3.4GHz (option) Intel Core i7 3.5GHz (option)
Form factor	ATX
Chipset	Intel C216
Bus	PCI, 32-bit/33MHz
Memory	2048MB DDR3 RAM 4096MB (option)
Graphics	Intel HD Graphics 400P onboard
USB	4 x USB 3.0 and 1 x USB 2.0 at front 6 x USB 2.0 internal
Ethernet	2 x Gigabit at front
Serial Ports (for baud rates up to 115kb/s only)	1 x RS232/422/485 at front 1 x RS232/422/485 and 4 x RS232 internal
Keyboard & mouse	1 x PS/2 at front
BIOS	American Megatrend Inc. (AMI)
Number of slots for I/O modules	3 PCI 4 x PCIe 1 x Mini PCIe

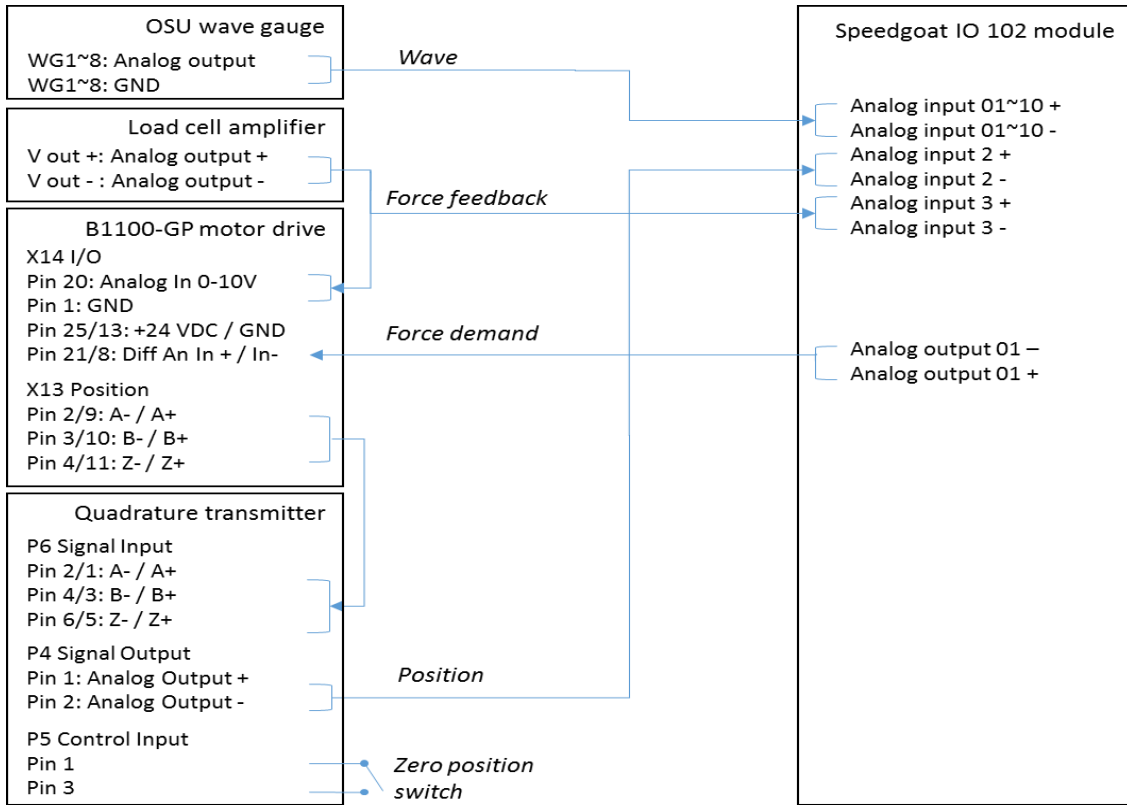
Drives	
Standard (for storing real-time application, Simulink Real-Time kernel, and logged data)	1 x 60GB SSD (read transfer rates up to 450MB/s, write transfer rates up to 450MB/s)
Options:	500GB or 1TB HDD 256GB SSD (read transfer rates up to 540MB/s, and write transfer rates of up to 520MB/s)
Power	
Power inlet	AC 100-240V, 50/60Hz, at rear
Power switch	at rear
Secondary power switch	at front
Reset button	none (secondary power switch)
Power LED	at front (combined with secondary power switch)
Environment	
Temperature	0° to +60°C (operating)
Humidity	10-90%, non-condensing
Software	
OS / RTOS	FreeDOS / Simulink Real-Time™ kernel, preinstalled on CompactFlash or Hard Disk for current release of MathWorks software
Development computer	Utilities for kernel transfer, I/O drivers and Simulink test models for your selected I/O modules

2. IO 102 module

Physical	
Form factor	PMC
Power requirements	+5VDC \pm 0.2 VDC at 1.4 Amps, maximum, 0.9 Amps typical
PCI bus	32bit / 33MHz
Connector	68-way SCSI3 Cable connectors: Tyco Electronics Board connector: Tyco Electronics part no. 5749069-7
Environmental	
Operating temperature	0 to 70°C (extended temperature variant: -40°C to +85°C)
Relative humidity	0 to 95%, non-condensing
Analog inputs (at 25°C)	
Number of inputs	Standard variant: 32 input lines, configurable as 32 single-ended or 16 differential channels, one A/D converter for all channels HV variant: 16 input lines, configurable as 16 single-ended or 8 differential channels, one A/D converter for all channels
Resolution	16 Bits (0.0015 percent of FSR)
Channel conversion time	3.3 μ s, maximum
Sampling mode	Sequential; 2, 4, 8, 16, or 32 channels per scan (32 channels available only in single-ended mode)
Voltage Ranges	Driver configurable as \pm 10V, \pm 5V or \pm 2.5V (HV variant: \pm 60V, \pm 30V or \pm 15V)
Input impedance	1M Ω line-to-ground, 2M Ω line-to-line, in parallel with 100pF (HV variant: 180K line-to-ground)
Bias current	80nA, maximum
Crosstalk rejection	85dB, DC-10kHz
Signal/Noise ratio (SNR)	80dB typical
Common mode rejection	60dB DC-60Hz, differential input mode
Over voltage protection	\pm 30V with power applied, \pm 15 Volts with power removed (HV variant: \pm 70 Volts).
DC accuracy (maximum composite error after autocalibration)	Standard variant: \pm 10V range: \pm 3.2mV (midscale accuracy), \pm 4.2mV (full scale accuracy) \pm 5V range: \pm 2.3mV (midscale accuracy), \pm 2.8mV (full scale accuracy) \pm 2.5V range: \pm 1.6mV (midscale accuracy), \pm 2mV (full scale accuracy) HV variant: \pm 60V range: \pm 30mV (midscale accuracy), \pm 6% of range (full scale accuracy) \pm 30V range: \pm 17mV (midscale accuracy), \pm 6% of range (full scale accuracy) \pm 15V range: \pm 10mV (midscale accuracy), \pm 6% of range (full scale accuracy)
Integral nonlinearity	\pm 0.003 percent FSR (FSR = fullscale range; e.g.: 20V on \pm 10V range)
Differential nonlinearity	\pm 0.0015 percent FSR

Analog outputs (at 25°C)	
Configuration	4 single-ended output channels
Resolution	16 Bits (0.0015 percent of FSR)
Settling time	8 μ s to 1LSB, typical 50% fullscale step
Voltage ranges	Same as selected for analog inputs: ± 10 , ± 5 or ± 2.5 V
Output resistance	1.0 Ohm maximum at I/O connector pins
Output protection	Withstands sustained short-circuiting to ground
Load current	Zero to ± 3 mA per channel
Load capacitance	Stable with 0 to 2000pF shunt capacitance
Noise	1.0mV-RMS, 10Hz-1MHz typical
Glitch Impulse	5 nV-Sec, typical on ± 2.5 V range
DC Accuracy (Max error, no-load):	± 10 V range: ± 2.7 mV (midscale accuracy), ± 3 mV (full scale accuracy) ± 5 V range: ± 1.9 mV (midscale accuracy), ± 2.3 mV (full scale accuracy) ± 2.5 V range: ± 1.3 mV (midscale accuracy), ± 1.7 mV (full scale accuracy)
Crosstalk rejection	85 dB minimum, DC - 1000 Hz
Integral nonlinearity	± 0.004 percent of FSR, maximum
Differential nonlinearity	± 0.0015 percent FSR
Digital I/O (at 25°C)	
Ports	16 bidirectional lines, configurable in groups of 8
Levels	Standard TTL
Output load	8mA

APPENDIX D: INSTRUMENTATION WIRING



APPENDIX F: LINMOT-TALK SETTING

1) Motor Wizard

Step 5/9; Additional Load Mass 1308 g

Step 7/9; Speed: 0.01 m/s, Mode: Actual Position

Step 8/9; Distance A: 750 mm

Step 9/9; HP: 0 mm, IP: 0 mm

2) Force feedback control setting

Project tree window: Parameters > Motion control SW > Protected Technology Functions > Analog Force Feedback Control

> Input Selection: Analog Input On X14.20

> Analog Force Feedback Config

0 V: -183.7 N (negative)

10 V: 157.8 N (positive)

Note: values are from calibration slope, but it should be tuned to have zero measured force at neutral position. (To check measured force, go to the Project tree windows: Variables > MC SW Force Control)

> Force Control Parameters

P Gain: 0.2 A/N

I Gain: 2 A/(N*s)

3) Command table setting (X14.16)

Entry ID: 10

Motion Command Type: VAI Go To Pos With Higher Force Ctrl Limit and Target Force

Target Position: -20 mm

Max. Velocity: 0.01 m/s

Acceleration: 0.1 m/s²

Force Limit: -0.9 N

Target Force: -1 N

4) Encoder setting for position (LT61QD)

Running a IS2 program after connecting a RS232 cable between the encoder and PC.

Output type: +/- 10 V

Output reading range: +/- 3000 (During the TEST III, it is changed to +/- 300 with 100 um resolution value of encoder simulation in LinMot-talk)

5) Force control operating

After homing the motor (check both 0. Switch on and 11. Home) first, uncheck the 11. Home of override value side.

After that, check both X14.16 in IO panel. If the motor is now in force control mode, the 9. Special Motion Active in Status window indicates on (1).

APPENDIX G: TEST RUNS

1) TEST CAMPAIGN I

Full Scale	Input		
Run#	Wave Height (m)	Wave Period (s)	Comments
20	1	5	Excitation Test
21	1	7	Excitation Test
22	1	9	Excitation Test
23	1	11	Excitation Test
24	1	13	Excitation Test
25	1	15	Excitation Test
26	1	17	Excitation Test
27	1	11	Excitation Test
28	1	5	Excitation Test
30			Free-Decay Test
40	1	9	Linear Damping
41	1	7	Linear Damping
42	1	11	Linear Damping
52	1	11	MPC
53	1	13	MPC
54	1	15	MPC
55	1	17	MPC

2) TEST CAMPAIGN II

Full Scale	Input			
Run#	Wave Height (m)	Wave Period (s)	Linear Damping	Comments
703	1	5	100000	Linear Damp.
704	1	5	200000	Linear Damp.
705	1	5	300000	Linear Damp.
706	1	5	400000	Linear Damp.
707	1	5	500000	Linear Damp.
708	1	7	300000	Linear Damp.

709	1	7	400000	Linear Damp.
710	1	7	500000	Linear Damp.
711	1	7	600000	Linear Damp.
712	1	7	1000000	Linear Damp.
713	1	9	700000	Linear Damp.
714	1	9	800000	Linear Damp.
715	1	9	900000	Linear Damp.
716	1	9	1000000	Linear Damp.
717	1	9	1100000	Linear Damp.
718	1	11	1100000	Linear Damp.
719	1	11	1200000	Linear Damp.
720	1	11	1300000	Linear Damp.
721	1	11	1400000	Linear Damp.
722	1	13	1500000	Linear Damp.
723	1	13	1400000	Linear Damp.
724	1	13	1300000	Linear Damp.
725	1	13	1200000	Linear Damp.
726	1	15	1700000	Linear Damp.
727	1	15	1800000	Linear Damp.
728	1	15	1900000	Linear Damp.
729	1	17	2000000	Linear Damp.
730	1	17	2100000	Linear Damp.
731	1	17	2200000	Linear Damp.
732	1	7	700000	Linear Damp.
733	1	7	800000	Linear Damp.
734	1	9	1200000	Linear Damp.
735	1	11	1500000	Linear Damp.
736	1	13	1100000	Linear Damp.
737	1	15	1600000	Linear Damp.
738	1	15	2000000	Linear Damp.
739	1	15	2100000	Linear Damp.
740	1	15	2200000	Linear Damp.
741	1	13	1600000	Linear Damp.

742	1	5	1000000	Linear Damp.
743	1	11	1000000	Linear Damp.
744	1	13	1000000	Linear Damp.
745	1	15	1000000	Linear Damp.
746	1	17	1000000	Linear Damp.
802	1	5		Causal control
803	1	7		Causal control
804	1	9		Causal control
805	1	11		Causal control
806	1	13		Causal control
807	1	15		Causal control
808	1	17		Causal control
900	1	11		Linear MPC
901	1	13		Linear MPC
902	1	13		Linear MPC
903	1	15		Linear MPC
904	1	17		Linear MPC
905	1	5		Linear MPC
906	1	7		Linear MPC
907	1	9		Linear MPC
908	1	11		Linear MPC
910	1	7		Uni-MPC
911	1	9		Uni-MPC
912	1	11		Uni-MPC
913	1	13		Uni-MPC
914	1	15		Uni-MPC
915	1	17		Uni-MPC
916	1	5		Uni-MPC
920	1	7		Uni-MPC (Neg)
921	1	9		Uni-MPC (Neg)
922	1	11		Uni-MPC (Neg)
923	1	13		Uni-MPC (Neg)
924	1	15		Uni-MPC (Neg)

925	1	17		Uni-MPC (Neg)
926	1	5		Uni-MPC (Neg)
930	1	7		Nonlinear (opt2)
931	1	9		Nonlinear (opt2)
932	1	11		Nonlinear (opt2)
933	1	13		Nonlinear (opt2)
934	1	15		Nonlinear (opt2)
935	1	5		Nonlinear (opt2)
940	1	7		Nonlinear (opt4)
941	1	9		Nonlinear (opt4)
942	1	11		Nonlinear (opt4)
943	1	5		Nonlinear (opt4)
944	1	7		Nonlinear (opt4)
945	1	9		Nonlinear (opt4)
946	1	11		Nonlinear (opt4)
947	1	13		Nonlinear (opt4)
948	1	15		Nonlinear (opt4)

3) TEST CAMPAIGN III

Full Scale	Input			
Run#	Wave Height (m)	Wave Period (s)	Damping (Ns/m)	Comments
H=1m				
6026	1	5	150000	Linear Damp.
6000	1	5	200000	Linear Damp.
6036	1	5	238476	Linear Damp.
6034	1	5	250000	Linear Damp.
6035	1	5	300000	Linear Damp.
6061	1	6	402436	Linear Damp.
6037	1	7	400000	Linear Damp.
6001	1	7	500000	Linear Damp.
6038	1	7	569476	Linear Damp.
6039	1	7	600000	Linear Damp.

6040	1	7	700000	Linear Damp.
6062	1	8	749936	Linear Damp.
6041	1	9	800000	Linear Damp.
6002	1	9	900000	Linear Damp.
6042	1	9	940976	Linear Damp.
6043	1	9	1000000	Linear Damp.
6044	1	9	1100000	Linear Damp.
6063	1	10	1117436	Linear Damp.
6045	1	11	1100000	Linear Damp.
6046	1	11	1200000	Linear Damp.
6003	1	11	1300000	Linear Damp.
6047	1	11	1400000	Linear Damp.
6048	1	11	1500000	Linear Damp.
6064	1	12	1482436	Linear Damp.
6049	1	13	1550000	Linear Damp.
6004	1	13	1600000	Linear Damp.
6050	1	13	1650976	Linear Damp.
6051	1	13	1700000	Linear Damp.
6052	1	13	1750000	Linear Damp.
6065	1	14	1824936	Linear Damp.
6053	1	15	1900000	Linear Damp.
6054	1	15	1950000	Linear Damp.
6005	1	15	2000000	Linear Damp.
6055	1	15	2050000	Linear Damp.
6056	1	15	2100000	Linear Damp.
6066	1	16	2136936	Linear Damp.
6057	1	17	1950000	Linear Damp.
6006	1	17	2000000	Linear Damp.
6058	1	17	2312476	Linear Damp.
6059	1	17	2500000	Linear Damp.
6060	1	17	2550000	Linear Damp.
H=2m				
6007	2	5	2000000	Linear Damp.

6008	2	7	500000	Linear Damp.
6009	2	9	900000	Linear Damp.
6010	2	11	1300000	Linear Damp.
6011	2	13	1600000	Linear Damp.
6012	2	15	2000000	Linear Damp.
6019	1	5		Linear MPC
6073	1	6		Linear MPC
6020	1	7		Linear MPC
6074	1	8		Linear MPC
6014	1	9		Linear MPC
6075	1	10		Linear MPC
6015	1	11		Linear MPC
6076	1	12		Linear MPC
6016	1	13		Linear MPC
6077	1	14		Linear MPC
6017	1	15		Linear MPC
6078	1	16		Linear MPC
6018	1	17		Linear MPC
6019	1	5		Linear MPC (re-run sim.)
6020	1	7		Linear MPC (re-run sim.)
6014	1	9		Linear MPC (re-run sim.)
6015	1	11		Linear MPC (re-run sim.)
6016	1	13		Linear MPC (re-run sim.)
6017	1	15		Linear MPC (re-run sim.)
6018	1	17		Linear MPC (re-run sim.)
6019	1	5		Linear MPC (re-run sim.)
6020	1	7		Linear MPC (re-run sim.)
6014	1	9		Linear MPC (re-run sim.)
6015	1	11		Linear MPC (re-run sim.)
6016	1	13		Linear MPC (re-run sim.)
6017	1	15		Linear MPC (re-run sim.)
6018	1	17		Linear MPC (re-run sim.)
6086	1	5		Linear MPC (Uni-Pos)

6087	1	7		Linear MPC (Uni-Pos)
6088	1	9		Linear MPC (Uni-Pos)
6089	1	11		Linear MPC (Uni-Pos)
6090	1	13		Linear MPC (Uni-Pos)
6091	1	15		Linear MPC (Uni-Pos)
6092	1	17		Linear MPC (Uni-Pos)
6079	1	5		Nonlinear MPC (opt 4)
6080	1	7		Nonlinear MPC (opt 4)
6081	1	9		Nonlinear MPC (opt 4)
6082	1	11		Nonlinear MPC (opt 4)
6083	1	13		Nonlinear MPC (opt 4)
6084	1	15		Nonlinear MPC (opt 4)
6085	1	17		Nonlinear MPC (opt 4)
6093	1	5		Nonlinear MPC (opt 2)
6094	1	7		Nonlinear MPC (opt 2)
6095	1	9		Nonlinear MPC (opt 2)
6096	1	11		Nonlinear MPC (opt 2)
6097	1	13		Nonlinear MPC (opt 2)
6098	1	15		Nonlinear MPC (opt 2)
6099	1	17		Nonlinear MPC (opt 2)
6068	1	5	$\alpha=4, \gamma=1e2$	Causal (re-run)
6028	1	7	$\alpha=1, \gamma=2e4$	Causal
6071	1	9	$\alpha=4, \gamma=1e2$	Causal (re-run)
6030	1	11	$\alpha=4, \gamma=1e2$	Causal
6031	1	13	$\alpha=2, \gamma=5e1$	Causal
6032	1	15	$\alpha=2, \gamma=5e1$	Causal
6033	1	17	$\alpha=2, \gamma=5e1$	Causal
6200	1	9	756600	Irregular (Lin. Damping)
6201	1	11	1013600	Irregular (Lin. Damping)
6205	1	9		Irregular (Linear MPC)
6206	1	11		Irregular (Linear MPC)